Functional characterization of eicosanoid signaling in *Drosophila* development

Daiki Fujinaga[1], Cebrina Nolan[1,2], and Naoki Yamanaka[1,*]

[1]Department of Entomology, Institute for Integrative Genome Biology, University of California, Riverside, Riverside, CA 92521, USA

[2]Current address: Institute for Molecular Bioscience, The University of Queensland, Brisbane, QLD 4072, Australia

*Corresponding author: Naoki Yamanaka, naoki.yamanaka@ucr.edu

Short title: Eicosanoid signaling in *Drosophila* development

Abstract

20-carbon fatty acid-derived eicosanoids are versatile signaling oxylipins in mammals. In particular, a group of eicosanoids termed prostanoids are involved in multiple physiological processes, such as reproduction and immune responses. Although some eicosanoids such as prostaglandin E2 (PGE2) have been detected in some insect species, molecular mechanisms of eicosanoid synthesis and signal transduction in insects have not been thoroughly investigated. Our phylogenetic analysis indicated that, in clear contrast to the presence of numerous receptors for oxylipins and other lipid mediators in humans, the *Drosophila* genome only possesses a single ortholog of such receptors, which is homologous to human prostanoid receptors. This G protein-coupled receptor, named Prostaglandin Receptor or PGR, is activated by PGE2 and its isomer PGD2 in *Drosophila* S2 cells. *PGR* mutant flies die as pharate adults with insufficient tracheal development, which can be rescued by supplying high oxygen. Consistent with this, through a comprehensive mutagenesis approach, we identified a *Drosophila* PGE synthase whose mutants show similar pharate adult lethality with hypoxia responses. *Drosophila* thus has a highly simplified eicosanoid signaling pathway as compared to humans, and it may provide an ideal model system for investigating evolutionarily conserved aspects of eicosanoid signaling.

Author Summary

There are numerous bioactive lipids that control animal physiology, and some of them are commonly observed in both humans and insects. Well-studied insects such as fruit flies can therefore be an excellent gateway to learn about lipid molecules that have common functions in various animal species. In this study, we analyzed the fruit fly genome to look for genes that encode sensors (or receptors) for such lipid molecules called lipid mediators and found that the fruit fly only has one such receptor, as compared to ~50 receptors in humans. Interestingly, the fly receptor we found was similar to human receptors for lipid molecules called prostanoids. Our work on the fruit fly prostanoid receptor further revealed that it is important for development of the fly respiratory system, and we showed that flies can also synthesize prostanoids in their body just like humans. Prostanoids are clinically important due to their pro-inflammatory functions, and some widely used drugs such as ibuprofen target enzymes that synthesize prostanoids. Our study on fruit fly prostanoids therefore provides a solid basis for using this simple organism to reveal common prostanoid functions in animals, which may provide important insights into animal health in general.

Introduction

Eicosanoids are 20-carbon fatty acid-derived bioactive lipids that regulate multiple biological processes such as inflammation and reproduction in animals [1,2]. Eicosanoids are synthesized in response to both external and internal stimuli including injury, infection, and gestation cycle, and induce various biological responses [3]. For example, a subclass of eicosanoids termed prostanoids (prostaglandins, thromboxanes, and prostacyclins) are known as strong inflammation-inducing factors in mammals [4,5]. Prostanoids are synthesized from arachidonic acid (AA), a 20-carbon polyunsaturated fatty acid, through reactions mediated by multiple biosynthetic enzymes [2,6] and exert their biological functions by interacting with G protein-coupled receptors (GPCRs) [4]. Because of the pro-inflammatory functions of prostanoids, prostanoid biosynthetic enzymes are important targets of a class of widely used drugs known as non-steroidal anti-inflammatory drugs or NSAIDs [7,8].

In insects, several prostanoids, mainly prostaglandins, have been reported in some species [9,10]. Through applications of synthetic ligands and biosynthesis inhibitors, functions of prostanoids in insect immune responses, hemocyte migration, and ovarian development have been reported [11–13]. Recently, a GPCR has been identified as a prostaglandin E2 (PGE2) receptor that mediates its immunomodulatory activities in a few lepidopteran species [14,15]. Targeted knockdown of putative prostanoid synthases has also been shown to reduce prostanoid production as well as immune responses in a lepidopteran insect [16,17], providing first examples of genetic loss-of-function studies of eicosanoid signaling in insects.

In the fruit fly *Drosophila melanogaster*, genes that are potentially involved in prostaglandin signaling have been mostly studied in the context of follicle maturation and border cell migration in the ovaries [11,18,19]. However, to the best of our knowledge, prostaglandin molecules have

rarely been reported in *D. melanogaster* to date, except a few studies that detected PGE2 immunoreactivity in adult fly homogenates [20,21] and various eicosanoid metabolites in the adult hemolymph [22]. Some studies even argue that *D. melanogaster* is unable to synthesize C20 oxylipins [23–25], and a C18 oxylipin-mediated inflammatory response pathway has been proposed [25]. Combined with the lack of information regarding any oxylipin receptors in *D. melanogaster*, our knowledge on eicosanoid signaling pathways in this important model organism is critically limited.

In the present study, we identified a single eicosanoid receptor-encoding gene in the *Drosophila* genome and investigated its functions during development. This GPCR, named Prostaglandin Receptor (PGR), can be activated by prostanoids *in vitro*, consistent with the fact that it is orthologous to mammalian prostanoid receptors. Detailed loss-of-function analyses and rescue experiments revealed that PGR is required for development of the adult tracheal system during metamorphosis. Moreover, through a comprehensive mutagenesis approach, we identified a PGE synthase that functions in the trachea and mediates local prostaglandin signaling that promotes adult tracheogenesis. Our study thus sets a solid basis and provides essential genetic tools for studying this highly conserved lipid signaling pathway in an important model organism.

58 **Results**

59 **CG7497/PGR is a single prostanoid receptor in *D. melanogaster***

60 We first compared amino acid sequences of all Class A GPCRs in *D. melanogaster* and
61 *Homo sapiens* to identify candidate receptors for lipid mediators in *D. melanogaster* (Fig 1A, S1
62 Table). Most fly receptors were clustered in accordance with their cognate ligands, and a single
63 *Drosophila* receptor, CG7497, was clustered with *H. sapiens* prostanoid receptors. CG7497
64 orthologs are also conserved in other insect species (S1 Fig, S2 Table), and its lepidopteran
65 orthologs have recently been reported as insect PGE2 receptors [14,15]. In contrast, no other
66 *Drosophila* GPCRs were found orthologous to other human lipid mediator receptors, such as
67 leukotriene B4 receptors and lysophosphatidic acid receptors (Fig 1A and 1B). This result
68 suggests that insects have highly simplified eicosanoid signaling mediated by a single GPCR. In
69 order to determine ligands for CG7497, the aequorin-based calcium mobilization assay was
70 performed using *Drosophila* S2 cells. Aequorin, a calcium-dependent luminescent protein, and
71 Gα15, a promiscuous G protein, were transfected into S2 cells along with a GPCR-containing
72 vector (either CG7497 or *H. sapiens* PGE2 receptor HsEP2) or an empty vector (Mock). By
73 quantifying calcium-dependent aequorin luminescence as a readout of Gα15-coupled GPCR
74 activation [26], it was confirmed that CG7497 was strongly activated by PGE2 or PGD2, while it
75 was only slightly activated by PGF2α, U46619 (thromboxane A2 analog), or iloprost
76 (prostacyclin analog) [27,28] (Fig 1C). These results indicate that CG7497 is a single *Drosophila*
77 prostanoid receptor that can be activated by a wide variety of prostanoids, particularly PGD2 and
78 PGE2. Hereafter, we call CG7497 PGR.

Fig 1. Identification of a prostanoid receptor in *D. melanogaster*.
(A) Unrooted maximum-likelihood phylogenetic tree of class A G protein-coupled receptors (GPCRs) in *H. sapiens* and *D. melanogaster*. GPCRs in *D. melanogaster* are indicated by blue branches, whereas branches for *H. sapiens* GPCRs are color-coded based on different classes of ligands. The scale bar indicates an evolutionary distance of 0.5 amino acid substitutions per site. Opsins and leucine-rich repeat containing GPCRs are not included in the phylogenetic tree. Accession numbers of the receptors analyzed are listed in S1 Table. (B) List of lipid mediator receptors in *H. sapiens* and their *Drosophila* orthologs. (C) Luminescence responses of S2 cells co-expressing *Aequorin* and *Gα15*, along with *CG7497/PGR* or *H. sapiens* PGE2 receptor *EP2* (*HsEP2*), to prostanoids or their synthetic analogs. Relative luminescence normalized by luminescence in ligand-free controls is shown. Cells expressing *CG7497/PGR* were significantly activated by all ligands, whereas cells expressing *EP2* were activated only by PGE2. n = 3. $*p < 0.05$, $**p < 0.01$, $***p < 0.001$ (Dunnett's test *vs* mock treatment control).

79

80 **PGR is required in tracheal cells for normal pupa-adult development**

81 *PGR* expression pattern was visualized using *PGR-Gal4* generated by the CRISPR-mediated
82 integration cassette system [29], where *T2A-Gal4* and 3xP3-GFP-encoding sequence were
83 inserted in the *PGR* locus, so that Gal4 is expressed under the control of the endogenous *PGR*
84 promoter (S2A Fig). *PGR* expression was detected in multiple tissues during *Drosophila*
85 development (Figs 2A and S3). In adults, it is expressed in the gonads, gut, dorsal vessel, and
86 hemocytes, as well as in the tracheae (Fig 2B). In particular, *PGR* is expressed in the tracheae in
87 all developmental stages tested, suggesting its important functions in regulating development of
88 the tracheal system. Indeed, *PGR* knockdown in the tracheae or terminal tracheal cells (TTCs)
89 caused pharate adult lethality or eclosion defects (Fig 2B), suggesting that *PGR* expression in
90 tracheal cells is necessary for normal progression of pupa-adult development.

Fig 2. Expression of *PGR* during development.
(A) Expression patterns of *CG7497*/*PGR* as visualized by *PGR-Gal4*-driven expression of *UAS-mCD8::GFP*. *PGR* is expressed in the prothoracic gland (outlined by the dashed line and marked by an arrow) and neurons located on the posterior end of the ventral nerve cord (indicated by an arrowhead) in third instar larvae. *PGR* is also expressed in the pupal and adult tracheae (dorsal trunks are indicated by dashed lines), as well as in testes, ovaries, dorsal vessel (indicated by an arrow), gut, and hemocytes in adults. Pupae are 48 hours after puparium formation, and adults are 72 hours after eclosion. Note the strong background GFP signals in the larval central nervous system (CNS) and adult optic lobes due to the *3xP3-GFP* marker in the *PGR-Gal4* line. Systemic GFP expression at different developmental stages is shown in S3 Fig. (B) Developmental phenotype caused by two independent *PGR* RNAi lines. *PGR* knockdown caused lethal phenotype at the pharate adult stage when induced either ubiquitously *(tubP-Gal4*), in *PGR* expression sites (*PGR-Gal4*), in tracheal cells (*btl-Gal4*), or in terminal tracheal cells (*dSRF-Gal4*). Numbers above the bars indicate flies analyzed for each genotype. Expression patterns of *Gal4* drivers are described in S11 Table. ***$p < 0.001$ (Chi-square test *vs* + > *PGR* RNAi with Bonferroni correction). Scale bars, 200 μm; 10 μm in the hemocyte images.

91

92 **PGR promotes adult tracheogenesis**

93 We next generated *PGR* knockout flies using the CRISPR-Cas9 system. Two mutant strains
94 generated by independent guide RNA (gRNA) pairs are expected to be null mutants, as their
95 exons are almost completely deleted (Fig 3A). Homozygous and transheterozygous *PGR* mutants
96 died during late pupa-adult development after wing pigmentation, similar to its trachea-specific
97 knockdown flies (Figs 3B and 3C). The lethal phenotype was significantly rescued by restoring
98 *PGR* expression in TTCs using *dSRF-Gal4* (Fig 3D). Although *PGR* overexpression in all
99 tracheal cells by *btl-Gal4* did not rescue the lethality, more adult flies eclosed when *PGR* was
100 overexpressed using both *btl-Gal4* and *dSRF-Gal4* in the transheterozygous mutant background.

101 These results suggest that *PGR* expression in tracheal cells, particularly in TTCs, is necessary for
102 normal development. Consistent with this, *PGR* knockout caused underdevelopment of the adult
103 tracheal system in the abdomen (Figs 3E and 3F). Length of tracheoles in the *PGR* mutants was
104 significantly shorter than control, indicating that PGR is necessary for promoting adult tracheal
105 development. Similar defects in tracheal development were observed when the tracheae were
106 visualized by GFP using another tracheal driver, *Trh-Gal4* (S4A and S4B Figs). Moreover,
107 overexpression of *PGR* in the tracheae and TTCs using *btl-Gal4* and *dSRF-Gal4* significantly
108 rescued underdeveloped tracheoles in *PGR* mutants (S4C and S4D Figs). Expression of hypoxia
109 response genes, *Lactate dehydrogenase* (*Ldh*) and *HIF prolyl hydroxylase* (*Hph*), was
110 upregulated in the *PGR* mutants, consistent with their defective tracheal development (Figs 3G
111 and 3H). The high expression of the hypoxia response genes in the *PGR* mutants was suppressed
112 by restoring *PGR* expression in TTCs (Figs 3G and 3H), in line with the developmental rescue
113 experiments. Altogether, these results indicate that PGR regulates adult tracheal development,
114 which is necessary for sufficient oxygen supply during pupa-adult development.

Fig 3. Phenotypic analysis of *CG7497/PGR* mutants.

(A) Schematic diagram of target sites of mutation on the *CG7497*/*PGR* locus. Two mutant alleles were generated using two pairs of different gRNAs. Genomic sequences of the mutants are shown in S1 Document. (B) Representative images of a developmentally arrested transheterozygous *PGR* mutant at the pharate adult stage. (C) Developmental phenotype of the *PGR* mutants. Most homozygous and transheterozygous *PGR* knockout flies died as pharate adults. ***$p < 0.001$ (multiple comparison Chi-square test with Bonferroni correction). Numbers above the bars indicate flies analyzed in each genotype. (D) Rescue of transheterozygous *PGR* mutants by *Gal4*-driven expression of *UAS-PGR*. The pharate adult lethality was rescued by overexpressing *PGR* either ubiquitously (*tubP-Gal4*), in *PGR* expression sites (*PGR-Gal4*), or in TTCs (*dSRF-Gal4*). ***$p < 0.001$ (Chi-square test *vs* + > *PGR* with Bonferroni correction). As *PGR-Gal4* is a loss of function allele of *PGR*, the transheterozygous mutant of PGR^{Gal4}/PGR^{B1} was used when restoring *PGR* expression using *PGR-Gal4*. Numbers above the bars indicate flies analyzed for each genotype. (E) The tracheae were visualized by *btl-Gal4*-driven expression of *UAS-mCD8::GFP* in the third (A3) and fourth (A4) abdominal segments at 72 hours after puparium formation (APF). (F) Total tracheal length in the third (A3) and fourth (A4) abdominal segments in selected areas. The transheterozygous *PGR* mutant showed defective tracheal development in both segments. n = 10. ***$p < 0.001$ (Student's *t*-test). (G, H) Relative expression levels of hypoxia response genes, *Lactate dehydrogenase* (*Ldh*) (G) and *HIF prolyl hydroxylase* (*Hph*) (H), in *PGR* mutants at 72 hours APF. Transheterozygous *PGR* mutants showed higher expression of the hypoxia response genes. High expression of the hypoxia response genes in *PGR* mutants was suppressed by expressing *PGR* either ubiquitously (*tubP-Gal4*), in *PGR* expression sites (*PGR-Gal4*), or in TTCs (*dSRF-Gal4*). Expression levels are normalized by the levels of a reference gene, *rp49*, in the same cDNA samples and shown as relative to $PGR^{A1/+}$. n = 3–8. ***$p < 0.001$ (among w^{1118}, $PGR^{A1/+}$ and $PGR^{A1/B1}$, Tukey's honestly significant difference test). *$p < 0.05$, **$p < 0.01$, ***$p < 0.001$ (Rescue by *PGR* overexpression, Dunnett's test *vs* $PGR^{A1/+}$). Scale bars, 200 μm in B and E.

115

116 **PGR promotes tracheogenesis during early pupal stages to provide oxygen required for**
117 **pupa-adult development**

118 In order to determine the exact timing of PGR requirement in adult tracheal development,
119 detailed expression analysis of hypoxia response genes in the *PGR* mutants was conducted (Fig
120 4A and 4B). Expression of both *Ldh* and *Hph* in the *PGR* mutants was higher than control flies
121 beginning at 16 hours after puparium formation (APF). Since pupation happens approximately at
122 12 hours APF, PGR seems to function immediately after pupation to promote adult tracheal
123 development. To further confirm this, a temporal knockdown experiment using a temperature-
124 sensitive Gal4 suppressor, Gal80^{ts}, was conducted (Fig 4C). At 18°C, flies pupate at about 24
125 hours APF. When *PGR* knockdown in the tracheae was initiated by 30 hours APF by transferring
126 animals from 18°C to 29°C, most flies died before eclosion. However, the lethality gradually
127 decreased as the onset of knockdown was shifted up to 48 hours APF, after which no significant
128 pupal lethality was observed. Likewise, in a temporal rescue experiment of the *PGR* mutants by
129 overexpressing *PGR*, most flies eclosed when the overexpression was initiated before 24 hours
130 APF. However, the lethality was increased as the onset of overexpression was shifted up to 57
131 hours APF, after which no significant rescue happened. These results indicate that PGR is
132 required for tracheogenesis during early stages of pupa-adult development after pupation.

Fig 4. Stage-specific requirement of *PGR* during pupa-adult development.
(A, B) Relative expression levels of hypoxia response genes, *Ldh* (A) and *Hph* (B), in *PGR* mutants between 0 and 96 hours after puparium formation (APF). Insects pupated about 12 hours APF. Homozygous and transheterozygous *PGR* mutants showed higher expression of both genes as compared to the heterozygous control after 16 hours APF. Expression levels are normalized by the levels of a reference gene, *rp49*, in the same cDNA samples and shown as relative to $PGR^{A1/+}$ at 0 hours APF. n = 3–6. $^{**}p < 0.01$, $^{***}p < 0.001$ (Dunnett's test *vs* $PGR^{A1/+}$). (C) Developmental deficiency caused by *PGR* RNAi using *btl-Gal4* and *tubP-Gal80^{ts}*. Insects were reared at 18°C and transferred to 29°C at indicated hours APF. Flies pupated at ~24 hours APF at 18°C. $^{*}p < 0.05$, $^{***}p < 0.001$ (upper panel, multiple comparison Chi-square test with Bonferroni correction; lower panel, Chi-square test *vs* 24 hours APF with Bonferroni correction). Numbers above the bars indicate flies analyzed for each treatment. (D) Rescue of the transheterozygous *PGR* mutant by *PGR-Gal4*-driven temporal expression of *UAS-PGR*. Insects were reared at 18°C and transferred to 29°C at indicated hours APF. $^{**}p < 0.01$, $^{***}p < 0.001$ (upper panel, multiple comparison Chi-square test with Bonferroni correction; lower panel, Chi-square test *vs* 24 hours APF with Bonferroni correction). Numbers above the bars indicate flies analyzed for each treatment. (E) Rescue of *PGR* mutants by high oxygen condition. Animals were kept in a container with 40% O_2 from indicated stages until eclosion. $^{*}p < 0.05$, $^{**}p < 0.01$, $^{***}p < 0.001$ (multiple comparison Chi-square test with Bonferroni correction). Numbers above the bars indicate flies analyzed for each treatment. (F) Principal component analysis based on whole body transcriptome of w^{1118} and $PGR^{A1/A1}$ at selected hours APF. mRNA components showed similar patterns between w^{1118} and $PGR^{A1/A1}$ from 0 hours until 48 hours APF, whereas different patterns were observed thereafter.

As the *PGR* mutants exhibited the hypoxia response due to defects in adult tracheal development, we reasoned that their developmental defects can be recovered by high concentrations of oxygen. We therefore transferred the *PGR* mutants to a growth chamber containing 40% oxygen at different stages of development (Fig 4E). More than half of the mutants eclosed when they were transferred to 40% oxygen by the mid pupal stage. Some flies

138 eclosed even when they were transferred to 40% oxygen during late pupa-adult development,
139 although the rescue rates were lower. This result confirmed that the *PGR* mutants die due to
140 insufficient oxygen supply caused by defective tracheogenesis during pupa-adult development.
141 Under normal oxygen concentration, the *PGR* mutants show no discernible developmental
142 defects up to the mid pupal stage and eventually die at the pharate adult stage. Consistent with
143 this observation, the whole-body transcriptome analysis revealed that gene expression patterns in
144 control and the *PGR* mutants are similar until mid pupa-adult development (48 h APF; Fig 4F).
145 In contrast, the *PGR* mutants showed distinct gene expression patterns at 72 and 96 hours APF.
146 Overall, these results suggest that PGR functions between pupation and mid pupa-adult
147 development to induce adult tracheal development, whose deficiency causes developmental
148 defects in late pupal stages due to insufficient oxygen supply and leads to pharate adult lethality.
149

150 **Prostaglandins are synthesized in *D. melanogaster***

151 What are the endogenous ligands for PGR that promote adult tracheogenesis in *D.*
152 *melanogaster*? In mammals, multiple active eicosanoids are synthesized from AA (Fig 5A).
153 Although there is no obvious cyclooxygenase (PGG/H synthase or COX) ortholog among ten
154 heme peroxidases conserved in insects [30] (S5 Fig, S3 Table), one heme peroxidase has been
155 proposed to function as COX in *D. melanogaster* [11]. Moreover, based on our phylogenetic
156 analyses, PGD, PGE, and PGF synthases are highly conserved in insects, although *D.*
157 *melanogaster* lacks some of them (Figs 5B and S6–S10, S4–S8 Tables). On the other hand,
158 among multiple cytochrome P450 enzymes in insects, there are no obvious orthologous enzymes
159 of CYP5A1 (thromboxane A synthase) or CYP8A1 (prostacyclin synthase) (S11 Fig, S9 Table).
160 These results suggest that prostaglandins are the major eicosanoids in insects. Indeed, PGD,

161 PGE, and PGF have been detected in some insects [31,32], including *D. melanogaster* [22].
162 Since PGR signaling in tracheogenesis is critically required during early pupal stages, we
163 reasoned that active PGR ligands are synthesized in the same time window during *Drosophila*
164 development. Therefore, Eicosanoid contents were analyzed in the whole-body extract of early
165 pupae by liquid chromatography-tandem mass spectrometry (LC-MS/MS). Under normal rearing
166 conditions, ~0.13 ng of AA was detected per animal, whereas prostanoids were undetectable. In
167 contrast, when larvae were reared on the food supplemented with AA, significant amounts of
168 PGD2, PGE2, and PGF2α were detected, whereas no other prostanoids were observed (Fig 5C).
169 These results indicate that flies have the ability to synthesize PGD, PGE, and PGF, consistent
170 with the presence of multiple prostaglandin synthase orthologs. Considering the high activity of
171 PGD2 and PGE2 as PGR ligands (Fig 1C), it is conceivable that either PGD2 or PGE2 is an
172 endogenous PGR ligand that promotes tracheogenesis during pupa-adult development.

Fig 5. Conserved prostanoid synthases in *D. melanogaster*.
(A) Schematic diagram of prostanoid synthetic pathways. Multiple prostanoids are synthesized from arachidonic acid (AA) by different enzymes. (B) *Drosophila* enzymes orthologous to human prostanoid synthases were identified by phylogenetic analyses. Phylogenetic trees are shown in S5–S11 Figs. PGD, PGE, and PGF synthases are highly conserved in insects, although *D. melanogaster* lacks some of them. (C) Prostanoids detected in whole body extracts of pupae by liquid chromatography-tandem mass spectrometry (LC-MS/MS)-based lipidomics. AA was detected in intact pupae at 0–4 hours after pupation, whereas prostanoids were undetectable. PGD2, PGE2, and PGF2α were detected in pupae that were raised in AA-supplemented diet during larval development. Data shown are mean total amount of eicosanoids in the whole body per animal ± SEM. n = 4–5.

173

174 **Cytosolic Prostaglandin E synthase/p23 activates local prostaglandin signaling to promote**
175 **tracheogenesis**

176 In order to identify prostaglandin synthase(s) that are responsible for tracheal development,
177 we generated null mutants of six *Drosophila* orthologs of PGD and PGE synthases (S12 Fig).
178 Among these mutants, a triple knockout mutant of three paralogous genes, *Mgstl*, *CG33177*, and
179 *CG33178* (*Prostaglandin E synthase 1* or *PTGES1* orthologs) and a mutant of *cytosolic*
180 *Prostaglandin E synthase (cPges)/p23* (a *PTGES3* ortholog) showed pupal lethal phenotype (Fig
181 6A). In particular, most *cPges/p23* mutant animals died during pupa-adult development, although
182 more than half of them died without pigmentation (Fig 6B). Importantly, only *cPges/p23* mutant
183 pupae showed the hypoxia response after 24 hours APF (Figs 6C and 6D) similar to the *PGR*
184 mutants (Figs 4A and 4B), suggesting that cPges/p23 is the major PGE synthase that produces
185 PGR ligands during early pupa-adult development. It should be noted that cPges/p23, as well as
186 PTGES3 in vertebrates, functions as a co-chaperone. In mammals, PTGES3 acts as a component
187 of the heat shock protein 90 (Hsp90)-based chaperon complex and facilitates functions of its
188 target proteins such as the estrogen receptor [33]. *Drosophila* cPges/p23 also stabilizes Hsp90 by
189 acting as a co-chaperon [34]. This potentially explains the high lethality of the *cPges/p23* mutant
190 pupae, as Hsp90 has important functions in *Drosophila* development [35].

191

Fig 6. Functional characterization of a *Drosophila* PGE synthase.

(A) Developmental phenotype of PGD and PGE synthase ortholog mutants. Null mutant of *cPges*/*p23* and triple mutants of *Mgst*$^{-}$, *CG33177*, and *CG33178* died during pupa-adult development. Multiple comparison Chi-square test with Bonferroni correction was applied among *cPges*/*p23* mutants including the heterozygous control. ***$p < 0.001$. (B) Representative images of *cPges*/*p23* knockout flies. About 70% of flies died before wing pigmentation, whereas ~30% of flies died as pharate adults. Scale bar, 200 μm. (C, D) Relative expression levels of hypoxia response genes, *Ldh* (C) and *Hph* (D), in the PGD and PGE synthase ortholog mutants. The *cPges*/*p23* mutant showed high expression of hypoxia response genes at 24 and 48 hours after puparium formation (APF). Expression levels are normalized by the levels of a reference gene, *rp49*, in the same cDNA samples and shown as relative to 0 hours APF of *GstS1*$^{-}$. n = 3–8. $p < 0.001$ (Tukey's honestly significant difference test). (E) Rescue of the *cPges*/*p23* mutant by *Gal4*-driven expression of either *cPges*/*p23* or human *prostaglandin E synthase 3* (*HsPTGES3*). The lethal phenotype was rescued by overexpressing *cPges*/*p23* or *HsPTGES3* either ubiquitously (*tubP-Gal4*), in *PGR* expression sites (*PGR-Gal4*), in tracheal cells (*btl-Gal4*), or in the epidermis (*Eip71CD-Gal4*). **$p < 0.01$, ***$p < 0.001$ (Chi-square test *vs* + > *cPges*/*p23* or + > *HsPTGES3* with Bonferroni correction). (F) Developmental deficiency caused by *cPges*/*p23* RNAi. *cPges*/*p23* knockdown flies died during pupa-adult development when induced using either a ubiquitous driver *(tubP-Gal4*) or a combination of the tracheal cell (*btl-Gal4*) and epidermis (*Eip71CD-Gal4*) drivers. Lethality caused by *cPges*/*p23* RNAi in tracheal cells and epidermis was significantly rescued by 40% O_2. ***$p < 0.001$ (multiple comparison Chi-square test *vs* + > *cPges*/*p23* RNAi with Bonferroni correction, or 20% O_2 *vs* 40% O_2). (G) PGE2 conversion assay using *Drosophila* S2 cells. Arachidonic acid (AA) was added to the culture medium of S2 cells transfected with *cPges*/*p23* or *HsPTGES3* along with a *H. sapiens cyclooxygenase* (*HsCOX1* or *HsCOX2*), and PGE2 amount in the medium was determined. The basal levels of PGE2 immunoreactivity in all samples is likely due to the cross-reactivity of the antibody used in the assay. Increased PGE2 immunoreactivity was detected in *cyclooxygenase*-expressing cells regardless of *cPges*/*p23* or *HsPTGES3* transfection. n = 4. (H) Reduction of the PGE2 synthetic activity of S2 cells by knocking down endogenous *cPges*/*p23* expression. AA was added to the culture medium of S2 cells transfected with *HsCOX2* and treated with *cPges*/*p23* dsRNAs. PGE2 amount in the medium was determined. n = 2 (AA 0 μM) or n = 4 (AA 10 μM). ***$p < 0.001$ (Dunnett's test *vs EGFP* dsRNA-treated cells).

192 Tissue-specific overexpression of *cPges/p23* using either *PGR-Gal4*, *btl-Gal4*, or an
193 epidermis driver *Eip71CD-Gal4* rescued the lethal phenotype of the *cPges/p23* mutant (Fig 6E).
194 Consistent with this, *cPges/p23* knockdown using a combination of *btl-Gal4* and *Eip71CD-Gal4*
195 drivers caused high lethality, which was significantly rescued by high concentrations of oxygen
196 (Fig 6F). These results suggest that prostaglandins are synthesized in the epidermis and trachea
197 to activate PGR in TTCs, thus forming a local prostaglandin signaling network that promotes
198 tracheogenesis during early pupal stages.
199 In order to confirm that cPges/p23 functions as a PGE synthase, we performed an enzymatic
200 conversion assay using *Drosophila* S2 cells. As an intermediate of PGE2 synthesis,
201 prostaglandin H2 (PGH2), is unstable, human COXs were co-expressed with either *cPges/p23* or
202 human *PTGES3* to detect PGE2 synthesis from AA using the enzyme-linked immunosorbent
203 assay (ELISA) that is highly specific to PGE2 (S13A Fig). Interestingly, PGE2 synthesis was
204 detected without *cPges/p23* or human *PTGES3* transfection, suggesting high endogenous PGE2
205 synthase activities in S2 cells (Fig 6G). Therefore, we applied double-stranded RNA (dsRNA)
206 against *cPges/p23* to reduce expression of endogenous *cPges/p23* (S13B Fig). As a result, PGE2
207 production was significantly suppressed by *cPges/p23* knockdown, indicating that cPges/p23
208 functions as a PGE synthase in *D. melanogaster* (Fig 6H).
209

210 **Discussion**

211 In this study, we revealed that a single GPCR that we named PGR mediates prostaglandin
212 signaling essential for adult tracheal development in *D. melanogaster*. PGE2 is synthesized in
213 the trachea and epidermis by cPGES3/p23 and activates PGR in TTCs after pupation. This
214 PGE2-PGR signaling induces tracheal development, which provides sufficient oxygen supply
215 during pupa-adult development.

216 In mammals, there are numerous species of lipid mediators [3], which act through various
217 GPCRs as shown in Fig 1. In contrast, our phylogenetic analyses clearly indicate that, among
218 these lipid mediator GPCRs, only prostanoid receptors are conserved between mammals and
219 insects, suggesting evolutionarily conserved functions of prostanoids in the animal kingdom.
220 Among nine prostanoid receptors in *H. sapiens*, there is a considerable overlap of their cognate
221 ligands, as well as a significant amount of crosstalk between their downstream signaling
222 pathways [2]. Humans and other mammals thus have a highly complex prostanoid signaling
223 network. In contrast, although PGD2, PGE2, and PGF2α have been detected in multiple insect
224 species [22,31,32], our current study indicates that all of them likely act through a single
225 receptor, PGR. Alternatively, it is also possible that there are as-yet-unknown insect prostanoid
226 receptors that are not homologous to human lipid mediator receptors. Nonetheless, our
227 comprehensive phylogenetic analyses of prostanoid biosynthetic enzymes indicate that
228 prostaglandins are the primary, and potentially the only, prostanoids produced in insects (Fig 5).
229 Altogether, prostaglandin-PGR signaling represents the primary lipid mediator signaling that is
230 highly conserved in the animal kingdom, and our current study provides a solid basis as well as
231 useful genetic tools for using *D. melanogaster* as an extremely simple model system to
232 investigate this highly conserved signaling pathway.

233 Our phylogenetic study suggested that one PGD synthase and five PGE synthases are
234 conserved in *D. melanogaster*. To date, several prostaglandin synthetic enzymes have been
235 reported in insects [11,16,17]. A recent study in *D. melanogaster* suggested that cPges/p23
236 functions as a PGE synthase in the ovary [19], and our current study further confirmed its PGE
237 synthetic function. During pupa-adult development, cPGES/p23 synthesizes PGE2 in the
238 epidermis and tracheae to activate local PGR signaling, which is consistent with observations in
239 mammals that prostanoids act locally at the site of their production [2]. It is likely that this local,
240 paracrine nature of prostaglandin signaling keeps the whole-body prostaglandin titer below the
241 detection limit, unless extra AA is provided in the food (Fig 5C). When larvae were fed with the
242 AA-supplemented diet, we also detected PGD2 and PGF2α, as well as PGE2, in early pupae. Our
243 study thus confirms that *D. melanogaster* has the ability to synthesize PGD and PGF, which is
244 consistent with the presence of a PGD synthase ortholog (GstS1) in *D. melanogaster* (Fig 5B).
245 Although we could not find obvious PGF synthase orthologs, a recent study suggests that Aldo-
246 keto reductase 1B (Akr1B) functions as a *Drosophila* PGF synthase [19]. Functional
247 characterization of these putative prostaglandin synthases, including PGE synthase orthologs
248 other than cPGES/p23, is clearly warranted in future studies.
249 Although prostanoids are highly pleiotropic signaling molecules [2], most prostanoid studies
250 in insects have focused on their functions in immunity and reproduction [9–19,21,22]. To our
251 knowledge, this is the first study to demonstrate that prostaglandin signaling promotes tracheal
252 development in insects. A fibroblast growth factor named branchless (bnl) and its receptor
253 breathless (btl) have been well investigated as important signaling molecules for branching and
254 guidance of the tracheae in *D. melanogaster* [36]. Growth of TTCs is controlled by oxygen
255 demand, as hypoxia stimulates *bnl* expression in target tissues to promote tracheal outgrowth in

256 both larvae and adults [37–39]. In contrast, however, it is reported that *bnl* expression is not
257 upregulated under hypoxic conditions immediately after pupation [40]. Indeed, expression levels
258 of *bnl* in heterozygous and homozygous *PGR* mutants were almost the same until the pharate
259 adult stage (S14A Fig), even though homozygous *PGR* mutants exhibited hypoxia responses
260 throughout the pupal stage (Figs 4A and 4B). These results suggest that oxygen demand does not
261 activate bnl-btl signaling during the pupal stage, and prostaglandin signaling acts as an
262 alternative tracheogenic signaling pathway during pupa-adult development. Interestingly, *PGR*
263 mutant flies rescued by high oxygen supply no longer require high oxygen for their survival after
264 eclosion. This is likely due to the elevated bnl-btl signaling induced by hypoxia immediately
265 after eclosion (S14B Fig), which is largely suppressed within 24 hours (S14C Fig). Indeed, the
266 underdeveloped tracheal system in *PGR* mutants rescued by 40% oxygen quickly recovers to the
267 level of the control heterozygous mutants within 24 hours after eclosion (S14D Fig). Overall,
268 these results suggest that oxygen demand activates bnl-btl signaling in adult flies as previously
269 reported [36,39,40], which induces compensatory tracheogenesis in *PGR* mutant flies after
270 eclosion.

271 Considering that PGR is the only evolutionarily conserved prostanoid receptor in the
272 *Drosophila* genome, it is possible that PGR mediates all major prostanoid-related biological
273 processes in flies. Consistent with this, our transcriptome analysis revealed lower expression of
274 antimicrobial peptides and reproduction-related genes in *PGR* mutant prepupae and pharate
275 adults, respectively (S10 Table, S15 Fig), suggesting potential involvement of prostaglandin
276 signaling in immunity and reproduction. Results of our current study, along with the genetic
277 tools we developed, are expected to provide valuable resources for future studies to investigate

278 such pleiotropic functions of prostaglandin signaling beyond development, which may give us

279 insights into this highly conserved signaling pathway from evolutionary perspectives.

280

281 **Materials and methods**

282

283 **Flies**

284 Flies were raised at 25°C under 12 h-light and 12 h-dark photoperiod. The animals were fed
285 on standard cornmeal diet containing 6 g *Drosophila* agar type II (Genesee Scientific, #66-103),
286 100 g D-(+)-glucose (SIGMA, #G8270-25KG), 50 g inactive dry yeast (Genesee Scientific, #62-
287 106), 70 g yellow cornmeal (Genesee Scientific, #62-101), 6 ml propionic acid (SIGMA,
288 #402907-500ML), and 10 ml Tegosept (Genesee Scientific, #20-258) in 1,025 ml of water. The
289 control strain w^{1118} and transgenic flies were obtained from the Bloomington *Drosophila* Stock
290 Center (BDSC) and Vienna *Drosophila* Resource Center (VDRC) as shown in S11 Table.
291 Vectors to construct *UAS-PGR* and *UAS-cPges/p23* fly lines were obtained from the *Drosophila*
292 Genomic Resource Center (DGRC, UFO02753 and UFO02035; S12 Table). *pUAST-HsPTGES3*
293 was prepared from *pCMV6-HsPTGES3* from ORIGENE and cloned into the *pUAST* vector. All
294 new transgenic flies were generated by BestGene Inc. Gene deletion mutant flies were generated
295 using the CRISPR-Cas9 system: PGR^{A1} and PGR^{B1} were generated as described below, whereas
296 the other mutant strains were generated by WellGenetics Inc. using CRISPR-based homologous
297 recombination. Schematic diagrams and detailed sequences of the mutants are shown in S12 Fig
298 and S2-6 Documents, respectively. All mutants were analyzed after backcrossing with the w^{1118}
299 control strain at least 4 times to minimize potential effects of off-target mutations.

300

301 **Cell lines**

302 S2 cells used for aequorin luminescence assay and enzyme assays were obtained from DGRC
303 (S2-DRSC, stock number 181) and maintained in 75 cm^2 flask (VWR, #10062-860) in Shields

304 and Sang M3 insect medium (Sigma-Aldrich, #S3652-500ML) containing 10% Insect Medium
305 Supplement (Sigma-Aldrich, #I7267-100ML), 10% heat-inactivated fatal bovine serum (Gibco,
306 #10082147), and 1% penicillin-streptomycin solution (Thermo Fisher Scientific, #15140122).
307 Cells were incubated in a humidified incubator at 25°C.
308

309 **Phylogenetic tree analysis**

310 Unrooted maximum-likelihood phylogenetic trees were generated using MEGAX [41].
311 Amino acid sequences of class A GPCRs (except for opsins and leucine-rich repeat-containing
312 GPCRs) and eicosanoid synthases in *H. sapiens* and *D. melanogaster* were selected using HUGO
313 Gene Nomenclature Committee at the European Bioinformatics Institute
314 (https://www.genenames.org/) and Flybase [42], respectively. Entire amino acid sequences of the
315 receptors and enzymes in the silkmoth (*Bombyx mori*), western honey bee (*Apis mellifera*), red
316 flour beetle (*Tribolium casteneum*), pea aphid (*Acrythosiphon pisum*), and Nevada termite
317 (*Zootermopsis nevadensis*) were obtained from National Center for Biotechnology Information
318 database [43] using full length amino acid sequences of *H. sapiens* and *D. melanogaster* proteins
319 as queries. The protein names and GenBank accession numbers are listed in S1–9 Tables.
320

321 **Aequorin-based calcium mobilization assay in S2 cells**

322 Vectors for exogenous expression of *Aequorin*, *Gα15*, *CG7497/PGR*, and *HsEP2* in S2 cells
323 were generated from *pLV-CMV-aequorin* (VectorBuilder), *pCMV6-GNA15* (Genomics-online),
324 GH27361 (DGRC), and *pCMV6-HsEP2* (ORIGENE), respectively, and cloned into the
325 *pBRAcPA* vector. S2 cells at a density of 2 million cells in 4 mL of the culture medium were
326 seeded on a 60 mm petri dish (Falcon). Transfection of 1 μg of *pBRAcPA-Aequorin*, 2 μg of

327 *pBRAcPA-Gα15*, and 1 μg of *pBRAcPA* containing either *CG7497/PGR* or *HsEP2* was
328 performed 3 hours after seeding using Effectene Transfection Reagent (Qiagen, #301425)
329 following the manufacturer's protocol. After 3 days, 4.5 million cells in 2 mL of the assay
330 medium (Shields and Sang M3 insect medium containing 10% Insect Medium Supplement) were
331 transferred into a 6-well clear flat bottom multiple well plate (Corning). The cells were then
332 incubated with 5 μM of coelenterazine-h (Promega, #S2001) for 4 hours with gently shaking.
333 After adding 1 ml of the assay medium, 50 μl of the cells (approximately 7,500 cells) were
334 applied to a LUMIstar Omega microplate reader (BMG Labtech). In this system, the cells were
335 injected into 50 μl of the assay medium containing 200 μM of a prostaglandin or a prostanoid
336 analog (Cayman Chemical, PGD2, #12010; PGE2, #14010; PGF2α, #16010; U-46619, #16450;
337 iloprost, #18215). Luminescence was detected every 0.2 seconds from 5 seconds before injection
338 until 85 seconds after injection. Peak areas were calculated and normalized by areas obtained
339 with no ligand containing medium.
340
341 **Visualization of *UAS-GFP*-expressing tissues**
342 Developmental stages of flies were determined based on hours after egg laying (larvae),
343 puparium formation (pupae), or eclosion (adults). Tissues were carefully dissected in PBS. *PGR*
344 expressing tissues were visualized with *PGR-Gal4*-driven expression of *UAS-mCD8::GFP* [29].
345 GFP signals in the whole body and dissected tissues were observed using a SteREO
346 Discovery.V12 microscope (Zeiss). GFP signal in hemocytes and the adult tracheal system were
347 observed using a Zeiss Axio Imager M2 equipped with ApoTome.2 (Zeiss). SrpHemo-
348 3xmCherry was used as a marker for hemocytes [44]. Pupae at 72 hours APF were dissected for
349 observing dorsal tracheae [45]. Dissected dorsal tracheae were visualized by *btl-Gal4* or *Trh-*

350 *Gal4*-driven expression of *UAS-mCD8::GFP*. For the PGR rescue experiment (S4C and S4D
351 Figs), *UAS-mCD8::GFP* was driven by the combination of *SRF-Gal4* and *btl-Gal4*. Two 0.2 mm
352 × 0.2 mm areas in the third and fourth abdominal segments were selected in each image.
353 Tracheae were traced and the total tracheal length in each image was measured using Fiji with
354 NeuronJ plugin [46].
355
356 **Scoring of lethal stages**
357 Early pupae (up to 24 h APF) were collected and kept in *Drosophila* narrow vials (Genesee
358 Scientific) containing wet tissue at 25°C under 12 h-light and 12 h-dark photoperiod. Phenotypes
359 of flies were scored at 120 h after APF as either eclosion, eclosion defect, pharate adult lethal, or
360 pupal lethal without wing pigmentation (lethal during early to middle pupa-adult development).
361
362 **Generation of *PGR* mutants**
363 *PGR* mutant alleles (PGR^{A1} and PGR^{B1}) were generated using the CRISPR-Cas9 system as
364 previously reported [47] with slight modifications. Pairs of gRNA target sequences (20 bp) were
365 designed as shown in Fig 2A. Annealed oligonucleotides containing 20-bp target sequences (S13
366 Table) were inserted into the *pBFv-U6.2* or *pBFv-U6.2B* vector provided by the National
367 Institute of Genetics [48]. The fragment containing the *U6* promotor and first gRNA in *pBFv-*
368 *U6.2* was ligated into *pBFv-U6.2B* containing the second gRNA. Injection of plasmids and
369 generation of G1 mutant strains were performed by BestGene Inc. Genotyping of PGR^{A1} and
370 PGR^{B1} was conducted by PCR with extracted genomic DNA of flies with designed primers listed
371 in S13 Table. Genomic sequences of the mutants are shown in S1 Document.
372

373 **Total RNA extraction and quantitative reverse transcription (qRT)-PCR**

374 Four pupae were collected at each developmental stage in 1.5 mL tubes. Total RNA from
375 animals was extracted using TRIzol reagent (Invitrogen, #15596018) according to the
376 manufacture's protocol. Extracted RNA was further purified using the RNeasy mini kit (Qiagen,
377 #74104) and treated with RNase-Free DNase Set (Qiagen, #79254) following the recommended
378 protocols. cDNA was synthesized from 500 ng RNA with PrimeScript RT Master Mix (Takara
379 Bio) and diluted in 4x volume of TE buffer (10 mM Tris-HCl, 1 mM ethylenediamine-tetraacetic
380 acid, pH 8.0). Amounts of mRNA were quantified by qRT-PCR on CFX connect real-time PCR
381 detection system (Bio-Rad) with iQ SYBR Green Supermix (Bio-Rad, #1708882) using specific
382 primers listed in S13 Table. For absolute quantification of mRNAs, serial dilutions of *pGEM-T*
383 plasmids (Promega, #A3600) containing coding sequences of the target genes were used as
384 standards. Transcript levels were normalized by *rp49* levels in the same samples.

385

386 **Temporal *PGR* knockdown and overexpression**

387 Flies were raised at 18°C, and white pupae were transferred into *Drosophila* narrow vials
388 (Genesee Scientific) containing wet tissue. Flies were then transferred to 29°C at different stages
389 and reared until eclosion or for 4 days after transfer.

390

391 **Rescue of *PGR* mutants by high oxygen condition**

392 Prepupae and pupae were collected every 24 hours and kept in normal condition until
393 selected developmental timing. Animals were then transferred into plastic boxes, and oxygen
394 was supplied up to 40% every 24 hours. Lethal stages were scored after 120 hours APF as
395 described above.

396

397 **Transcriptome analysis**

398 Eggs of PGR^{A1} and w^{1118} were laid on grape juice plates. Newly hatched larvae were
399 transferred to standard cornmeal diet with less than 50 larvae/vials. Males and females were
400 separated during the 3rd instar stage, and heterozygous mutants were removed using GFP signals
401 in balancer-carrying larvae. Flies were transferred into vials containing wet tissue at puparium
402 formation and kept until selected hours APF. Four biological replicates for each genotype and
403 developmental timing (3 males and 3 females per sample) were collected and frozen in liquid
404 nitrogen. Total RNA was extracted with the TRIzol reagent and RNeasy mini kit as described
405 above. RNA qualification, library preparation, and RNA-seq were performed by Novogene Inc.
406 Briefly, RNA quality was analyzed using an Agilent Bioanalyzer 2100. mRNA enriched using
407 oligo(dT) beads was fragmented randomly, and cDNA was synthesized using mRNA template
408 and random hexamer primers. After sequencing adaptor ligation, libraries were analyzed with
409 NovaSeq 6000 (Illumina) to obtain 150-cycle paired-end sequencing, which produced more than
410 17.1 million reads per sample. Adaptor sequence-containing reads and low-quality reads were
411 removed with the fastp software [49]. Reads were then aligned to the *Drosophila* genome
412 (BDGP6.46, Ensembl) [50] with Hisat2 [51]. The number of aligned reads on each gene region
413 was counted with samtools [52] and featureCount [53]. Differential expression analysis and
414 principal component analysis were performed with DESeq2 packages using iDEP0.96
415 (http://bioinformatics.sdstate.edu/idep92/) [54]. Transcripts meeting a cutoff of 2-fold difference
416 in mRNA abundance and false discovery rate of < 5% were considered as differentially
417 expressed genes.

418

419 **Prostanoid detection**

420 Eggs of w^{1118} were laid on grape juice plates as described above. Newly hatched larvae were
421 transferred to cornmeal diet containing selected amounts of AA with less than 50 larvae/vials.
422 Fifty early pupae (0–4 hours after pupation) were collected in sample tubes and kept at -80°C
423 until analysis. Extraction and detection of eicosanoids were performed at the UCSD Lipidomics
424 Core. Briefly, 100 µl of 10% methanol with an internal standard mix (Cayman Chemical) was
425 added to each sample, and pupae were homogenized by a bead homogenizer. Homogenates were
426 then purified by polymeric reverse phase columns (Phenomenex, 8B-S100-UBJ) with 50 µl of
427 elution buffer (63% de-ionized water, 37% acetonitrile, and 0.02% Acedic Acid). Eicosanoid
428 determination was performed by reverse phase-ultra-performance liquid chromatography-tandem
429 mass spectrometry with ACQUITY UPLC System (Waters) and SCIEX 6500 triple quadrupole
430 linear ion trap mass spectrometer (AB Sciex) as described previously [55].

431

432 **Synthesis of *cPges*/*p23* double-stranded RNA**

433 PCR was carried out using primers containing T7 promotor sequences (listed in S13 Table)
434 using a *cPges*/*p23* cDNA clone LD23532 (DGRC) as a template. RNA was synthesized using
435 the MEGAscript T7 Transcription Kit (Ambion, AM1334), followed by incubation with DNase
436 for 30 min at 37°C. After incubation at 95°C for 5 min, the corresponding RNA products were
437 mixed and gradually cooled down to room temperature for annealing. Two pairs of dsRNAs
438 were prepared and purified using the RNeasy mini kit according to the manufacture's instruction.

439

440 **Enzymatic assay in S2 cells**

441 Vectors for exogenous expression of *HsCOX1*, *HsCOX2*, *cPges*/*p23*, and *HsPTGES3* in S2
442 cells were generated from *pCMV6-HsCOX1* (ORIGENE), *pCMV6-HsCOX2* (ORIGENE),
443 LD23532 (DGRC), and *pCMV6-HsPTGES3* (ORIGENE), respectively, and cloned into the
444 *pBRAcPA* vector. S2 cells at a density of 1 million cells in 2 ml of the culture medium were
445 seeded on a 6-well clear flat bottom multiple well plate (Corning). For enzyme overexpression
446 analysis, 0.5 µg of *pBRAcPA-COX1* or *pBRAcPA-COX2* and 0.5 µg of *pBRAcPA-cPges*/*p23* or
447 *pBRAcPA-HsPTGES3* were transfected as described above. For RNAi experiments, 0.5 µg of
448 *pBRAcPA-COX2* was transfected, and 10 µg of each *cPges*/*p23* dsRNA was added at the time of
449 transfection and every 24 hours afterward. After 2 days (overexpression) or 3 days (RNAi) of
450 incubation, 0.5 million cells in the assay medium were transferred into 24-well clear flat bottom
451 multiple well plate (Corning) and incubated for 18 hours. Cells were incubated with selected
452 concentrations of AA (Millipore-Sigma, #A3611) for 30 min, and then the amounts of PGE2 in
453 the culture medium were quantified using the Prostaglandin E2 ELISA Kit (Cayman, #514010)
454 using a VICTOR X3 luminometer (Perkin Elmer). For testing cross-reactivity of the anti-PGE2
455 antibody (S13A Fig), 5-hydroxyeicosatetraenoic acid (5-HETE; #34210), 9-HETE (#34400), 15-
456 HETE (#34700), 12-hydroxyheptadecatrienoic acid (#34590), 8(9)-eicosatrienoic acid (#50351),
457 and 11(12)-dihydroxyeicosatetraenoic acid (#51511) were obtained from Cayman Chemical.
458

459 **Data deposition**

460 Sequence data obtained by RNA-seq are available under BioProject accession number
461 PRJNA1126659 at the SRA (https://www.ncbi.nlm.nih.gov/sra).
462

463 **Conflict of interest**

464 The authors declare no competing interest.

465

466 **Acknowledgement**

467 We thank Vienna *Drosophila* Resource Center, Bloomington *Drosophila* Stock Center (NIH
468 P40 OD018537), T. Neufeld, and M.B. O'Connor for fly stocks; FlyBase (supported by NIH
469 U41 HG000739 and U24 HG010859) for providing curated *Drosophila* genome information,
470 S.H. Yamanaka, and M.E. Adams for sharing luminometers; Lipidomics core at the University of
471 California, San Diego for eicosanoid determination; *Drosophila* Genomics Resource Center
472 (NIH P40 OD010949) for cell lines; and *Drosophila* Genomics Resource Center and National
473 Institute of Genetics for vectors and cDNA clones. This study was supported by a Pew
474 Biomedical Scholars Award from the Pew Charitable Trusts to N.Y., a USDA NIFA Hatch
475 project CA-R-ENT-5094-H to N.Y., an NIH Director's New Innovator Award DP2 GM132929
476 to N.Y., and an NIH grant R35 GM153331 from NIGMS to N.Y.

477

478 **Author contributions**

479 Conceptualization, N.Y.; Methodology, D.F and N.Y.; Investigation, D.F. C.N., and N.Y;
480 Writing – Original Draft, D.F. and N.Y.; Writing – Review & Editing, D.F. and N.Y.;
481 Supervision, N.Y.; Funding Acquisition, N.Y.

482

483 **References**

484 1. Dennis E, Norris P. Eicosanoid storm in infection and inflammation. Nat Rev Immunol.
485 2015;15: 511–523 doi:10.1038/nri3859
486 2. Calder PC. Eicosanoids. Essays Biochem. 2020;64 (3): 423–441.
487 doi:10.1042/EBC20190083
488 3. Dyall SC, Balas L, Bazan NG, Brenna JT, Chiang N, da Costa Souza F et al.
489 Polyunsaturated fatty acids and fatty acid-derived lipid mediators: Recent advances in the
490 understanding of their biosynthesis, structures, and functions. Prog Lipid Res. 2022;86:
491 101165. doi:10.1016/j.plipres.2022.101165
492 4. Leuti A, Fazio D, Fava M, Piccoli A, Oddi S, Maccarrone M. Bioactive lipids,
493 inflammation and chronic diseases. Adv Drug Deliv Rev. 2020;159: 133–169.
494 doi:10.1016/j.addr.2020.06.028
495 5. Schmid T, Brüne B. Prostanoids and resolution of inflammation - Beyond the lipid-
496 mediator class switch. Front Immunol. 2021;12: 714042.
497 doi:10.3389/fimmu.2021.714042
498 6. Gabbs M, Leng S, Devassy JG, Monirujjaman M, Aukema HM. Advances in our
499 understanding of oxylipins derived from dietary PUFAs. Adv Nutr (Bethesda, Md.).
500 2015;6(5): 513–540. doi:10.3945/an.114.007732
501 7. Rainsford KD. 2007. Anti-inflammatory drugs in the 21st century. Sub-Cell Biochem.
502 2007;42: 3–27. doi:10.1007/1-4020-5688-5_1
503 8. Bacchi S, Palumbo P, Sponta A, Coppolino MF. Clinical pharmacology of non-steroidal
504 anti-inflammatory drugs: a review. Antiinflamm Antiallergy Agents Med. 2012;11(1):
505 52–64. doi:10.2174/187152312803476255

506 9. Stanley D. Prostaglandins and other eicosanoids in insects: biological significance. Annu
507 Rev Entomol. 2006;51: 25–44. doi:10.1146/annurev.ento.51.110104.151021
508 10. Stanley D, Kim Y. Prostaglandins and other eicosanoids in insects: Biosynthesis and
509 biological actions. Front Physiol. 2019;9: 1927. doi:10.3389/fphys.2018.01927
510 11. Tootle TL, Spradling AC. *Drosophila* Pxt: a cyclooxygenase-like facilitator of follicle
511 maturation. Development. 2008;135(5): 839–847. doi:10.1242/dev.017590
512 12. Stanley D, Kim Y. Prostaglandins and their receptors in insect biology. Front Endocrinol.
513 2011;2: 105. doi:10.3389/fendo.2011.00105
514 13. Ahmed S, Kim Y. PGE2 mediates cytoskeletal rearrangement of hemocytes via Cdc42, a
515 small G protein, to activate actin-remodeling factors in *Spodoptera exigua* (Lepidoptera:
516 Noctuidae). Arch Insect Biochem 2019;102(4): e21607. doi:10.1002/arch.21607
517 14. Kwon H, Yang Y, Kumar S, Lee DW, Bajracharya P, Calkins TL et al. Characterization
518 of the first insect prostaglandin (PGE2) receptor: *MansePGE2R* is expressed in
519 oenocytoids and lipoteichoic acid (LTA) increases transcript expression. Insect Biochem
520 Mol Biol. 2020;117: 103290. doi:10.1016/j.ibmb.2019.103290
521 15. Kim Y, Ahmed S, Al Baki MA, Kumar S, Kim K, Park Y et al. Deletion mutant of PGE2
522 receptor using CRISPR-Cas9 exhibits larval immunosuppression and adult infertility in a
523 lepidopteran insect, *Spodoptera exigua*. Dev Comp Immunol. 2020;111: 103743.
524 doi:10.1016/j.dci.2020.103743
525 16. Ahmed S, Stanley D, Kim, Y. An insect prostaglandin E2 synthase acts in immunity and
526 reproduction. Front Physiol. 2018;9: 1231. doi:10.3389/fphys.2018.01231
527 17. Sajjadian SM, Ahmed S, Al Baki MA, Kim Y. Prostaglandin D2 synthase and its
528 functional association with immune and reproductive processes in a lepidopteran insect,

529 *Spodoptera exigua*. Gen Comp Endocrinol. 2020;287: 113352.
530 doi:10.1016/j.ygcen.2019.113352
531 18. Fox EF, Lamb MC, Mellentine SQ, Tootle TL. Prostaglandins regulate invasive,
532 collective border cell migration. Mol Biol Cell. 2020;31(15): 1584–1594.
533 doi:10.1091/mbc.E19-10-0578
534 19. Mellentine SQ, Brown HN, Ramsey AS, Li J, Tootle TL. Specific prostaglandins are
535 produced in the migratory cells and the surrounding substrate to promote *Drosophila*
536 border cell migration. Front Cell Dev Biol. 2024;11: 1257751.
537 doi:10.3389/fcell.2023.1257751
538 20. Pagés M, Roselló J, Casas J, Gelpí E, Gualde N, Rigaud M. Cyclooxygenase and
539 lipoxygenase-like activity in *Drosophila melanogaster*. Prostaglandins. 1986;32(5): 729–
540 740. doi:10.1016/0090-6980(86)90195-4
541 21. Gong C, Guo Z, Hu Y, Yang Z, Xia J, Yang X et al. A horizontally transferred plant fatty
542 acid desaturase gene steers whitefly reproduction. Adv Sci. 2024;11(10): e2306653.
543 doi:10.1002/advs.202306653
544 22. Azizpor P, Okakpu OK, Parks SC, Chavez D, Eyabi F, Martinez-Beltran S et al.
545 Polyunsaturated fatty acids stimulate immunity and eicosanoid production in *Drosophila*
546 *melanogaster*. J Lipid Res. 2024;100608. doi:10.1016/j.jlr.2024.100608
547 23. Shen LR, Lai CQ, Feng X, Parnell LD, Wan JB, Wang JD et al. *Drosophila* lacks C20
548 and C22 PUFAs. J Lipid Res 2010;51(10): 2985–2992. doi:10.1194/jlr.M008524
549 24. Tan L, Xin X, Zhai L, Shen L. *Drosophila* fed ARA and EPA yields eicosanoids, 15S-
550 Hydroxy-5Z,8Z, 11Z, 13E-Eicosatetraenoic acid, and 15S-Hydroxy-5Z,8Z,11Z,13E,17Z-
551 eicosapentaenoic acid. Lipids. 2016;51(4): 435–449. doi:10.1007/s11745-016-4131-3

552 25. Kwon SY, Massey K, Watson MA, Hussain T, Volpe G, Buckley CD et al. Oxidised
553 metabolites of the omega-6 fatty acid linoleic acid activate dFOXO. Life Sci Alliance.
554 2020;3(2): e201900356. doi:10.26508/lsa.201900356
555 26. Thomsen W, Frazer J, Unett D. Functional assays for screening GPCR targets. Curr Opin
556 Biotechnol. 2005;16(6):655-665. doi:10.1016/j.copbio.2005.10.008.
557 27. Coleman RA, Humphrey PP, Kennedy I, Levy GP, Lumley P. Comparison of the actions
558 of U-46619, a prostaglandin H2-analogue, with those of prostaglandin H2 and
559 thromboxane A2 on some isolated smooth muscle preparations. Br J Pharmacol.
560 1981;73(3): 773–778. doi:10.1111/j.1476-5381.1981.tb16814.x
561 28. Schrör K, Darius H, Matzky R, Ohlendorf R. The antiplatelet and cardiovascular actions
562 of a new carbacyclin derivative (ZK 36 374)--equipotent to PGI2 *in vitro*. N-S Arch
563 Pharmacol. 1981;316(3): 252–255. doi:10.1007/BF00505658
564 29. Lee PT, Zirin J, Kanca O, Lin WW, Schulze KL, Li-Kroeger D et al. A gene-specific
565 T2A-GAL4 library for *Drosophila*. eLife. 2018;7: e35574. doi:10.7554/eLife.35574
566 30. Scarpati M, Qi Y, Govind S, Singh S. A combined computational strategy of sequence
567 and structural analysis predicts the existence of a functional eicosanoid pathway in
568 *Drosophila melanogaster*. PloS One. 2019;14(2): e0211897.
569 doi:10.1371/journal.pone.0211897
570 31. Büyükgüzel K, Tunaz H, Putnam SM, Stanley D. Prostaglandin biosynthesis by midgut
571 tissue isolated from the tobacco hornworm, *Manduca sexta*. Insect Biochem Mol Biol.
572 2002;32(4): 435–443. doi:10.1016/s0965-1748(01)00121-7

573 32. Tunaz H, Putnam SM, Stanley DW. Prostaglandin biosynthesis by fat body from larvae
574 of the beetle *Zophobas atratus*. Arch Insect Biochem Physiol 2002;49(2): 80–93.
575 doi:10.1002/arch.10008
576 33. Knoblauch R, Garabedian MJ. Role for Hsp90-associated cochaperone p23 in estrogen
577 receptor signal transduction. Mol Cell Biol. 1999;19(5): 3748-3759.
578 doi:10.1128/MCB.19.5.3748.
579 34. Tsuboyama K, Tadakuma H, Tomari Y. Conformational activation of argonaute by
580 distinct yet coordinated actions of the Hsp70 and Hsp90 chaperone systems. Mol Cell.
581 2018;70(4): 722–729.e4. doi:10.1016/j.molcel.2018.04.010
582 35. Ohhara Y, Hoshino G, Imahori K, Matsuyuki T, Yamakawa-Kobayashi K. The Nutrient-
583 responsive molecular chaperone Hsp90 supports growth and development in *Drosophila*.
584 Front Physiology. 2021;12: 690564. doi:10.3389/fphys.2021.690564
585 36. Hayashi S, Kondo T. Development and function of the *Drosophila* tracheal system.
586 Genetics. 2018;209(2): 367–380. doi:10.1534/genetics.117.300167
587 37. Jarecki J, Johnson E, Krasnow MA. Oxygen regulation of airway branching in
588 *Drosophila* is mediated by branchless FGF. Cell. 1999;99(2): 211–220.
589 doi:10.1016/s0092-8674(00)81652-9
590 38. Centanin L, Dekanty A, Romero N, Irisarri M, Gorr TA, Wappner P. Cell autonomy of
591 HIF effects in *Drosophila*: tracheal cells sense hypoxia and induce terminal branch
592 sprouting. Dev Cell. 2008;14(4): 547–558. doi:10.1016/j.devcel.2008.01.020
593 39. Tamamouna V, Rahman MM, Petersson M, Charalambous I, Kux K, Mainor H et al.
594 Remodelling of oxygen-transporting tracheoles drives intestinal regeneration and

595 tumorigenesis in *Drosophila*. Nature Cell Biol. 2021;23(5): 497–510.
596 doi:10.1038/s41556-021-00674-1
597 40. Li Y, Padmanabha D, Gentile LB, Dumur CI, Beckstead RB, Baker KD. HIF- and non-
598 HIF-regulated hypoxic responses require the estrogen-related receptor in *Drosophila*
599 *melanogaster*. PLoS Genet. 2013;9(1): e1003230. doi:10.1371/journal.pgen.1003230
600 41. Kumar S, Stecher G, Li M, Knyaz C, Tamura K. MEGA X: Molecular Evolutionary
601 Genetics Analysis across Computing Platforms. Mol Biol Evol. 2018;35(6): 1547–1549.
602 doi:10.1093/molbev/msy096
603 42. Gramates LS, Agapite J, Attrill H, Calvi BR, Crosby MA, Dos Santos G et al. FlyBase: a
604 guided tour of highlighted features. Genetics. 2022;220(4): iyac035.
605 doi:10.1093/genetics/iyac035
606 43. Sayers EW, Bolton EE, Brister JR, Canese K, Chan J, Comeau DC et al. Database
607 resources of the national center for biotechnology information. Nucleic Acids Res.
608 2022;50(D1): D20–D26. doi:10.1093/nar/gkab1112
609 44. Gyoergy A, Roblek M, Ratheesh A, Valoskova K, Belyaeva V, Wachner S et al. Tools
610 allowing independent visualization and genetic manipulation of *Drosophila*
611 *melanogaster* macrophages and surrounding tissues. G3 (Bethesda). 2018;8(3):845-857.
612 doi:10.1534/g3.117.300452.
613 45. Chen F. Preparation and immunofluorescence staining of the trachea in *Drosophila* larvae
614 and pupae. Bio-protocol. 2016;6(9): e1797. doi:10.21769/BioProtoc.1797.
615 46. Meijering E. Neuron tracing in perspective. Cytometry A. 2010;77(7): 693–704.
616 doi:10.1002/cyto.a.20895

617 47. Okamoto N, Viswanatha R, Bittar R, Li Z, Haga-Yamanaka S, Perrimon N, Yamanaka N.
618 A membrane transporter is required for steroid hormone uptake in *Drosophila*. Dev Cell.
619 2018;47(3): 294–305.e7. doi:10.1016/j.devcel.2018.09.012
620 48. Kondo S, Ueda R. Highly improved gene targeting by germline-specific Cas9 expression
621 in *Drosophila*. Genetics. 2013;195(3): 715–721. doi:10.1534/genetics.113.156737
622 49. Chen S, Zhou Y, Chen Y, Gu J. fastp: an ultra-fast all-in-one FASTQ preprocessor.
623 Bioinformatics. 2018;34(17), i884–i890. doi:10.1093/bioinformatics/bty560
624 50. Cunningham F, Allen JE, Allen J, Alvarez-Jarreta J, Amode MR, Armean et al. Ensembl
625 2022. Nucleic acids research. 2022;50(D1): D988–D995. doi:10.1093/nar/gkab1049
626 51. Kim D, Paggi JM, Park C, Bennett C, Salzberg SL. Graph-based genome alignment and
627 genotyping with HISAT2 and HISAT-genotype. Nature Biotechnol. 2019;37(8): 907–
628 915. doi:10.1038/s41587-019-0201-4
629 52. Danecek P, Bonfield JK, Liddle J, Marshall J, Ohan V, Pollard MO et al. Twelve years of
630 SAMtools and BCFtools. GigaScience. 2021;10(2): giab008.
631 doi:10.1093/gigascience/giab00
632 53. Liao Y, Smyth GK, Shi W. featureCounts: an efficient general purpose program for
633 assigning sequence reads to genomic features. Bioinformatics. 2014;30(7): 923–930.
634 doi:10.1093/bioinformatics/btt656
635 54. Ge SX, Son EW, Yao R. iDEP: an integrated web application for differential expression
636 and pathway analysis of RNA-Seq data. BMC Bioinformatics. 2018;19(1): 534.
637 doi:10.1186/s12859-018-2486-6

638 55. Quehenberger O, Armando AM, Brown AH, Milne SB, Myers DS, Merrill AH et al.
639 Lipidomics reveals a remarkable diversity of lipids in human plasma. J Lipid Res.
640 2010;51(11): 3299–3305. doi:10.1194/jlr.M009449
641

642 **Captions of supporting information**

643

644 **S1 Fig. Phylogenetic tree of insect class A GPCRs.**

645 Unrooted maximum-likelihood phylogenetic tree of class A GPCRs in *Drosophila melanogaster*,
646 *Bombyx mori*, *Apis mellifera*, *Tribolium castaneum*, *Acyrthosiphon pisum*, and *Zootermopsis*
647 *nevadensis*. CG7497/PGR orthologs are conserved in all insect species analyzed. The scale bar
648 indicates an evolutionary distance of 0.5 amino acid substitutions per site. Accession numbers of
649 the receptors analyzed are listed in S2 Table.

650

651 **S2 Fig. Characterization of the *PGR-Gal4* strain.**

652 (**A**) Schematic diagram of the PGR^{Gal4} allele [29]. *T2A-Gal4* is inserted in the first intron of *PGR*
653 along with the *3xP3-GFP* marker. (**B**) Developmental phenotype of the PGR^{Gal4} mutant. Most
654 homozygous and transheterozygous *PGR* mutants died as pharate adults, indicating the loss of
655 PGR function in PGR^{Gal4} flies. ***$p < 0.001$ (multiple comparison Chi-square test with
656 Bonferroni correction). Numbers above the bars indicate flies analyzed in each genotype.

657

658 **S3 Fig. Expression of *PGR* during development.**

659 Expression patterns of *PGR* visualized by *PGR-Gal4*-driven expression of *UAS-mCD8::GFP*.
660 Strong GFP signals were observed in the tracheae in all developmental stages tested. They were
661 also observed in oenocytes in larvae, pharate adults, and newly emerged adults as indicated by
662 arrows. Due to the *3xP3-GFP* marker in the *PGR-Gal4* line, background GFP signals are
663 observed in the larval CNS, larval gut, and adult eyes as indicated by arrowheads. Detailed

664 tissue-specific expression patterns are shown in Fig 2A. L1–L3, 1st, 2nd, and 3rd instar larvae;
665 AE, after eclosion. Scale bars: 200 μm.
666
667 **S4 Fig. Abdominal tracheae in *PGR* mutants visualized by *UAS-mCD8::GFP*.**
668 (**A**) Pupal abdominal tracheae in heterozygous and transheterozygous *PGR* mutants visualized by
669 *Trh-Gal4*-driven *UAS-mCD8::GFP* expression at 72 hours after puparium formation (APF). (**B**)
670 Total tracheal length in the third (A3) and fourth (A4) abdominal segments in the selected area as
671 visualized by *Trh-Gal4*-driven *UAS-mCD8::GFP* expression. Transheterozygous mutants
672 showed defective tracheal development in both segments. n = 8–9. ***$p < 0.01$ (Student's *t*-
673 test). (**C**) Pupal abdominal tracheae in heterozygous and transheterozygous *PGR* mutants
674 visualized by *btl-Gal4*- and *dSRF-Gal4*-driven *UAS-mCD8::GFP* expression at 72 hours APF.
675 Overexpression of *PGR* in the tracheae and TTCs partially rescued underdeveloped tracheoles in
676 *PGR* mutants. (**D**) Total tracheal length in A4 in the selected area as visualized by *btl-Gal4*- and
677 *dSRF-Gal4*-driven *UAS-mCD8::GFP* expression. Tracheal length in A3 was not measured due to
678 excessive GFP signals in A3 driven by *dSRF-Gal4*. n = 10–11. **$p < 0.1$, ***$p < 0.01$ (Tukey's
679 honestly significant difference test). Scale bars: 200 μm.
680
681 **S5 Fig. Phylogenetic tree of heme peroxidases in *H. sapiens* and insects.**
682 Unrooted maximum-likelihood phylogenetic tree of heme peroxidases in *Homo sapiens*,
683 *Drosophila melanogaster*, *Bombyx mori*, *Apis mellifera*, *Tribolium castaneum*, *Acyrthosiphon*
684 *pisum*, and *Zootermopsis nevadensis*. Branches are color-coded for different species.
685 Cyclooxygenases (PGG/H synthases) in *H. sapiens* are highlighted. The scale bar indicates an

686 evolutionary distance of 0.5 amino acid substitutions per site. Accession numbers of the enzymes
687 analyzed are listed in S3 Table.
688
689 **S6 Fig. Phylogenetic tree of glutathione S-transferases in *H. sapiens* and insects.**
690 Unrooted maximum-likelihood phylogenetic tree of glutathione S-transferases in *Homo sapiens*,
691 *Drosophila melanogaster*, *Bombyx mori*, *Apis mellifera*, *Tribolium castaneum*, *Acyrthosiphon*
692 *pisum*, and *Zootermopsis nevadensis*. Branches are color-coded for different species. Clades that
693 include PGD synthase and PGE synthase 1 in *H. sapiens* are highlighted. The scale bar indicates
694 an evolutionary distance of 0.5 amino acid substitutions per site. Accession numbers of the
695 enzymes analyzed are listed in S4 Table.
696
697 **S7 Fig. Phylogenetic tree of glutaredoxins in *H. sapiens* and insects.**
698 Unrooted maximum-likelihood phylogenetic tree of glutaredoxin domain-containing proteins in
699 *Homo sapiens*, *Drosophila melanogaster*, *Bombyx mori*, *Apis mellifera*, *Tribolium castaneum*,
700 *Acyrthosiphon pisum*, and *Zootermopsis nevadensis*. Branches are color-coded for different
701 species. The clade that includes PGE synthase 2 in *H. sapiens* is highlighted. The scale bar
702 indicates an evolutionary distance of 0.5 amino acid substitutions per site. Accession numbers of
703 the enzymes analyzed are listed in S5 Table.
704
705 **S8 Fig. Phylogenetic tree of carbonyl reductases in *H. sapiens* and insects.**
706 Unrooted maximum-likelihood phylogenetic tree of carbonyl reductases in *Homo sapiens*,
707 *Drosophila melanogaster*, *Bombyx mori*, *Apis mellifera*, *Tribolium castaneum*, *Acyrthosiphon*
708 *pisum*, and *Zootermopsis nevadensis*. Branches are color-coded for different species. The clade

709 that includes carbonyl reductase 1 (PGF synthase) in *H. sapiens* is highlighted. The scale bar
710 indicates an evolutionary distance of 0.5 amino acid substitutions per site. Accession numbers of
711 the enzymes analyzed are listed in S6 Table.
712
713 **S9 Fig. Phylogenetic tree of aldo-keto reductases in *H. sapiens* and insects.**
714 Unrooted maximum-likelihood phylogenetic tree of aldo-keto reductases in *Homo sapiens*,
715 *Drosophila melanogaster*, *Bombyx mori*, *Apis mellifera*, *Tribolium castaneum*, *Acyrthosiphon*
716 *pisum*, and *Zootermopsis nevadensis*. Branches are color-coded for different species. The clade
717 that includes aldo-keto reductase (PGF synthase 2) in *H. sapiens* is highlighted. The scale bar
718 indicates an evolutionary distance of 0.5 amino acid substitutions per site. Accession numbers of
719 the enzymes analyzed are listed in S7 Table.
720
721 **S10 Fig. Phylogenetic tree of peroxiredoxins in *H. sapiens* and insects.**
722 Unrooted maximum-likelihood phylogenetic tree of peroxiredoxins in *Homo sapiens*, *Drosophila*
723 *melanogaster*, *Bombyx mori*, *Apis mellifera*, *Tribolium castaneum*, *Acyrthosiphon pisum*, and
724 *Zootermopsis nevadensis*. Branches are color-coded for different species. The clade that includes
725 peroxiredoxin (PGF synthase) in *H. sapiens* is highlighted. The scale bar indicates an
726 evolutionary distance of 0.5 amino acid substitutions per site. Accession numbers of the enzymes
727 analyzed are listed in S8 Table.
728
729 **S11 Fig. Phylogenetic tree of cytochrome P450 enzymes in *H. sapiens* and insects.**
730 Unrooted maximum-likelihood phylogenetic tree of cytochrome P450 enzymes in *Homo sapiens*,
731 *Drosophila melanogaster*, *Bombyx mori*, *Apis mellifera*, *Tribolium castaneum*, *Acyrthosiphon*

732 *pisum*, and *Zootermopsis nevadensis*. Branches are color-coded for different species. The four
733 major CYP clans in insects are highlighted. There are no orthologous enzymes of Cyp5A1 or
734 Cyp8A1 in insects. The scale bar indicates an evolutionary distance of 0.5 amino acid
735 substitutions per site. Accession numbers of the enzymes analyzed are listed in S9 Table.
736
737 **S12 Fig. Mutagenesis of PGD/PGE synthase orthologs.**
738 Mutagenesis was conducted by CRISPR-Cas9-based homologous recombination to insert the
739 3xP3-RFP sequence into each target site. Two single guide RNAs (sgRNAs) were designed for
740 each target to delete entire coding sequences shown in orange. Genomic sequences of the
741 mutants are provided in S2–S6 Documents.
742
743 **S13 Fig. ELISA specificity and knockdown efficiency regarding the enzymatic conversion**
744 **assay in *Drosophila* S2 cells.**
745 (**A**) Cross-reactivity of the anti-PGE2 antibody used in the PGE2 ELISA system. Serial dilutions
746 of AA and various eicosanoids previously detected in the *Drosophila* hemolymph after AA
747 injection [22] were tested for their potential cross-reactivity. AA and PGF2α have 0.017% and
748 0.25% cross-reactivity, respectively. HETE, hydroxyeicosatetraenoic acid; HHTrE,
749 hydroxyheptadecatrienoic acid; EET, eicosatrienoic acid; DiHET, dihydroxyeicosatetraenoic
750 acid. (**B**) Relative expression levels of *cPges*/*p23* in S2 cells treated with dsRNA for 3 days.
751 *cPges*/*p23* mRNA levels were downregulated in *cPges*/*p23* RNAi cells as compared to the
752 negative control (*EGFP* RNAi). Expression levels are normalized by the levels of a reference
753 gene, *rp49*, in the same cDNA samples. n = 3. *$p < 0.05$, ** < 0.01 (Dunnett's test *vs EGFP*
754 RNAi).

755

756 **S14 Fig. Hypoxia response and tracheogenesis in *PGR* mutants.**

757 (**A**) Relative expression levels of *branchless* (*bnl*) in *PGR* mutants from 0 to 96 hours after
758 puparium formation (APF). Insects pupated about 12 hours APF. Homozygous mutant pupae did
759 not show significantly higher expression of *bnl* until 96 hours APF. (**B, C**) Relative expression
760 levels of hypoxia response genes (*Ldh* and *Hph*) and *bnl* in adult *PGR* mutants rescued by high
761 oxygen supply during pupa-adult development. Eclosed flies were transferred to the normal
762 oxygen condition within 2 hours after eclosion and kept there for 30 min (B) or 24 hours (C)
763 before RNA extraction. Rescued *PGR* mutant flies express high levels of *Ldh* and *Hph*
764 immediately after eclosion, which decreases within 24 hours. In contrast, *bnl* continues to be
765 highly expressed in *PGR* mutant flies 24 hours after eclosion. Expression levels are normalized
766 by the levels of a reference gene, *rp49*, in the same cDNA samples and shown as relative to
767 $PGR^{A1/+}$ at 0 hours APF. n = 3–4. $*p < 0.05$, $**p < 0.01$, $***p < 0.001$ (Student's *t*-test *vs*
768 $PGR^{A1/+}$). (**D**) Adult tracheal development in *PGR* heterozygous and transheterozygous mutants
769 raised under 40% oxygen during pupa-adult development. Abdominal tracheae in adult males
770 were visualized by *btl-Gal4*-driven *UAS-mCD8::GFP* expression within 2 hours or 24 hours
771 after eclosion. In newly emerged *PGR* transheterozygous mutants, the adult tracheal system was
772 underdeveloped, which recovered to the level of the control heterozygous mutants within 24
773 hours after eclosion. Scale bar: 200 μm.

774

775 **S15 Fig. Representative antimicrobial peptide and reproduction-related genes**
776 **downregulated in *PGR* mutants.**

777 Expression of antimicrobial peptide genes (A) and reproduction-related genes (B) in w^{1118}
778 control and the *PGR* mutant based on RNA-seq data. Expression levels of *Cecropin A1* and *A2*
779 (*CecA1* and *CecA2*), *Defensin* (*Def*), and *Drosomycin* (*Drs*) in the *PGR* mutant were
780 significantly lower than control at 0 hours after puparium formation (APF). Expression of *Sex*
781 *peptide receptor* (*SPR*), *Yolk protein 1* (*Yp1*), and *Yp2* in the *PGR* mutant was significantly
782 downregulated at 96 hours APF. Expression levels are shown as reads per kilobase of transcript
783 per million mapped reads (RPKM). $*p < 0.05$, $***p < 0.001$ (Student's *t*-test).
784
785 **S1 Table. GPCRs in the phylogenetic tree, related to Figs 1A and 1B.**
786
787 **S2 Table. GPCRs in the phylogenetic tree, related to S1 Fig.**
788
789 **S3 Table. Heme peroxidases in the phylogenetic tree, related to S4 Fig.**
790
791 **S4 Table. Glutathione S-transferases in the phylogenetic tree, related to S5 Fig.**
792
793 **S5 Table. Glutaredoxins in the phylogenetic tree, related to S6 Fig.**
794
795 **S6 Table. Carbonyl reductases in the phylogenetic tree, related to S7 Fig.**
796
797 **S7 Table. Aldo-keto reductases in the phylogenetic tree, related to S8 Fig.**
798
799 **S8 Table. Peroxiredoxins in the phylogenetic tree, related to S9 Fig.**

800

801 **S9 Table. Cytochrome P450 enzymes in the phylogenetic tree, related to S10 Fig.**

802

803 **S10 Table. Top affected gene functions in the *PGR* mutant.**

804

805 **S11 Table: *Drosophila* strains.**

806

807 **S12 Table: Plasmid constructs.**

808

809 **S13 Table: Primers and oligonucleotides.**

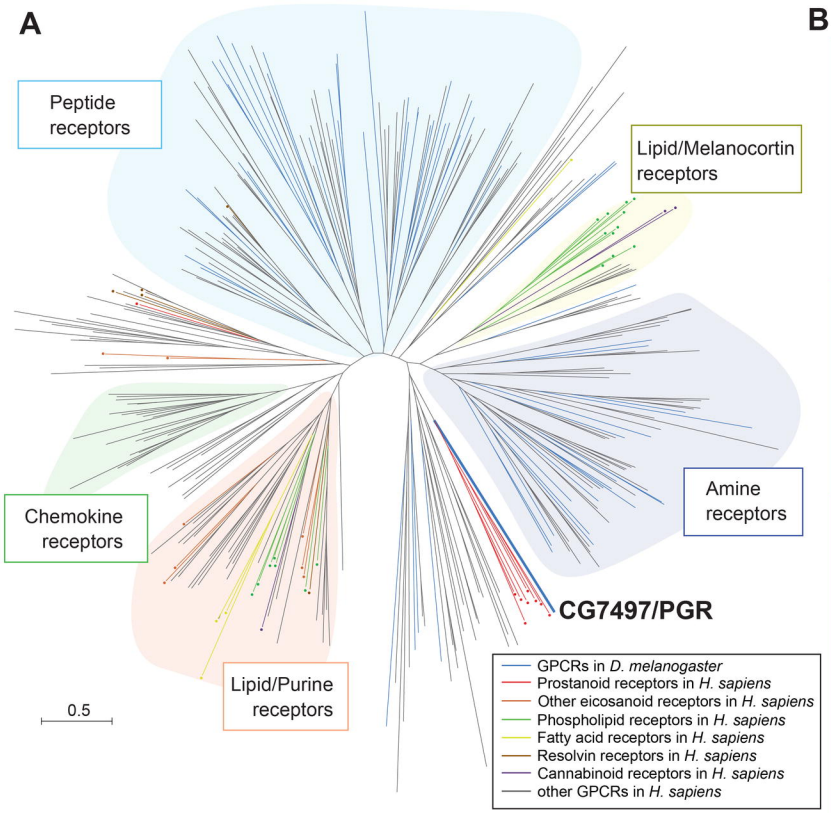

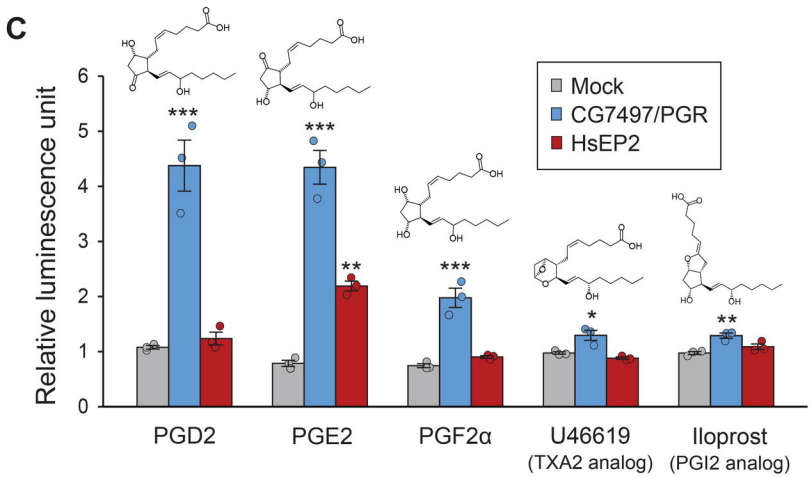

B

	Receptor in *H. sapiens*	Ortholog in *D. melanogaster*
Prostanoid receptors	Prostaglandin E2 receptor EP1	CG7497/PGR
	Prostaglandin E2 receptor EP2	CG7497/PGR
	Prostaglandin E2 receptor EP3	CG7497/PGR
	Prostaglandin E2 receptor EP4	CG7497/PGR
	Prostaglandin F2-alpha receptor	CG7497/PGR
	Thromboxane A2 receptor	CG7497/PGR
	Prostacyclin (PGI2) receptor	CG7497/PGR
	Prostaglandin D2 receptor DP1	CG7497/PGR
	Prostaglandin D2 receptor DP2	No ortholog
Other eicosanoid receptors	Leukotriene B4 receptor 1	No ortholog
	Leukotriene B4 receptor 2	No ortholog
	Cycteinyl leukotriene receptor 1	No ortholog
	Cycteinyl leukotriene receptor 2	No ortholog
	Uracil nucleotide/cycteinyl leukotriene receptor	No ortholog
	Oxoeicosanoid recptor 1	No ortholog
	12-Hydroxyeicosatetraenoic acid receptor	No ortholog
	2-oxoglutarate receptor 1	No ortholog
Phospho-lipid receptors	Lysophosphatidic acid receptor 1	No ortholog
	Lysophosphatidic acid receptor 2	No ortholog
	Lysophosphatidic acid receptor 3	No ortholog
	Lysophosphatidic acid receptor 4	No ortholog
	Lysophosphatidic acid receptor 5	No ortholog
	Lysophosphatidic acid receptor 6	No ortholog
	G-protein coupled receptor 34	No ortholog
	G-protein coupled receptor 174	No ortholog
	Pupative P2Y purinoceptor 10	No ortholog
	Sphingosine 1-phosphate receptor 1	No ortholog
	Sphingosine 1-phosphate receptor 2	No ortholog
	Sphingosine 1-phosphate receptor 3	No ortholog
	Sphingosine 1-phosphate receptor 4	No ortholog
	Sphingosine 1-phosphate receptor 5	No ortholog
	G-protein coupled receptor 3	No ortholog
	G-protein coupled receptor 6	No ortholog
	G-protein coupled receptor 12	No ortholog
	Platelet-activating factor receptor	No ortholog
Fatty acid receptors	Free fatty acid receptor 1	No ortholog
	Free fatty acid receptor 2	No ortholog
	Free fatty acid receptor 3	No ortholog
	Free fatty acid receptor 4	No ortholog
Pro-resolving mediator receptors	N-arachidonyl glycine receptor	No ortholog
	G-protein coupled receptor 32	No ortholog
	Chemokine-like receptor 1	No ortholog
	N-formyl peptide receptor	No ortholog
	G-protein coupled receptor 37	No ortholog
Cannabinoid receptors	Cannabinoid receptor 1	No ortholog
	Cannabinoid receptor 2	No ortholog
	G-protein coupled receptor 55	No ortholog

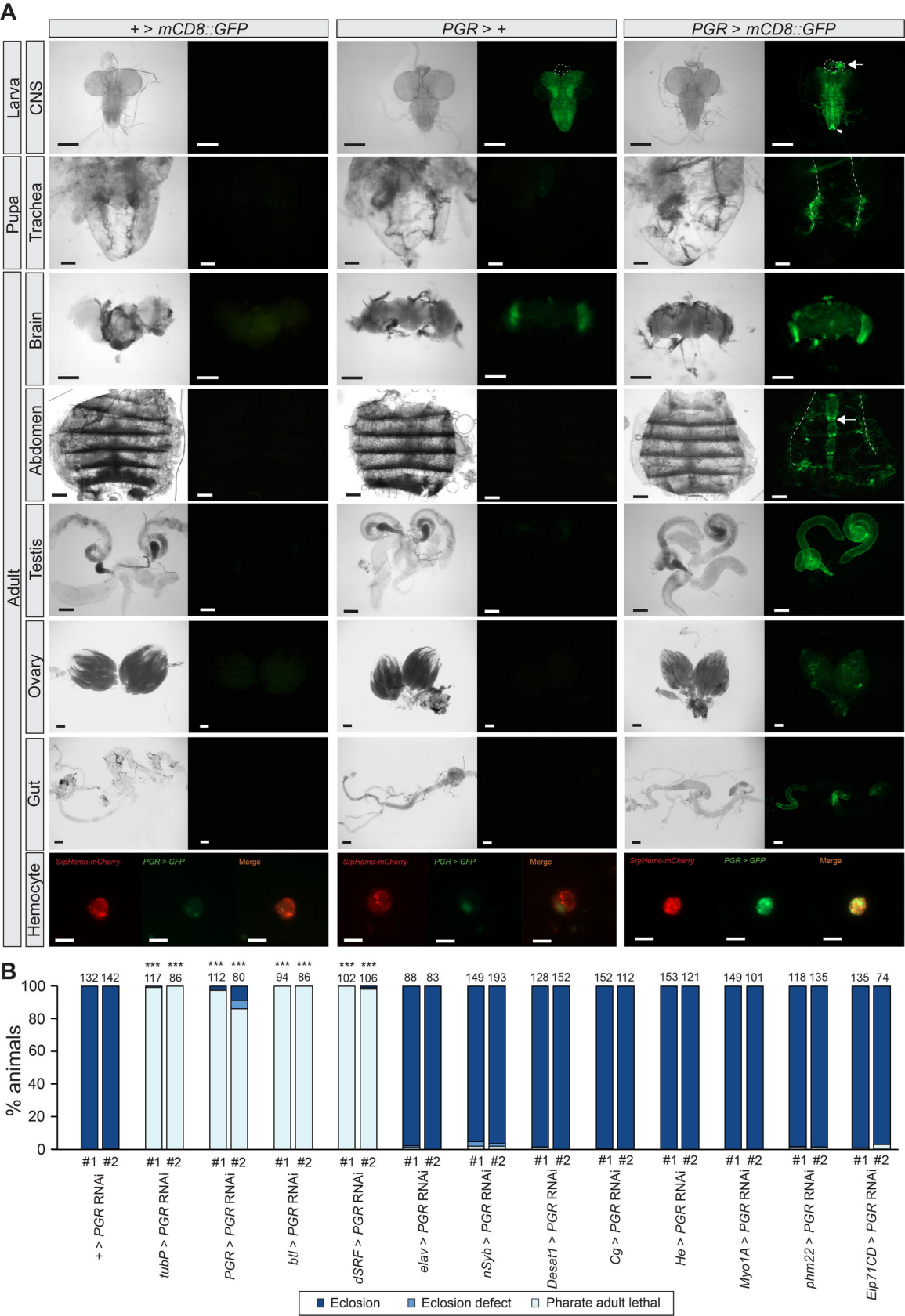
A
+ > mCD8::GFP
PGR > +
PGR > mCD8::GFP
Larva
CNS
Pupa
Trachea
Adult
Brain
Abdomen
Testis
Ovary
Gut
Hemocyte
SrpHemo-mCherry
PGR > GFP
Merge
B
% animals
100
80
60
40
20
0
132 142
117 86
112 80
94 86
102 106
88 83
149 193
128 152
152 112
153 121
149 101
118 135
135 74
***
#1 #2
+ > PGR RNAi
tubP > PGR RNAi
PGR > PGR RNAi
btl > PGR RNAi
dSRF > PGR RNAi
elav > PGR RNAi
nSyb > PGR RNAi
Desat1 > PGR RNAi
Cg > PGR RNAi
He > PGR RNAi
Myo1A > PGR RNAi
phm22 > PGR RNAi
Eip71CD > PGR RNAi
Eclosion
Eclosion defect
Pharate adult lethal

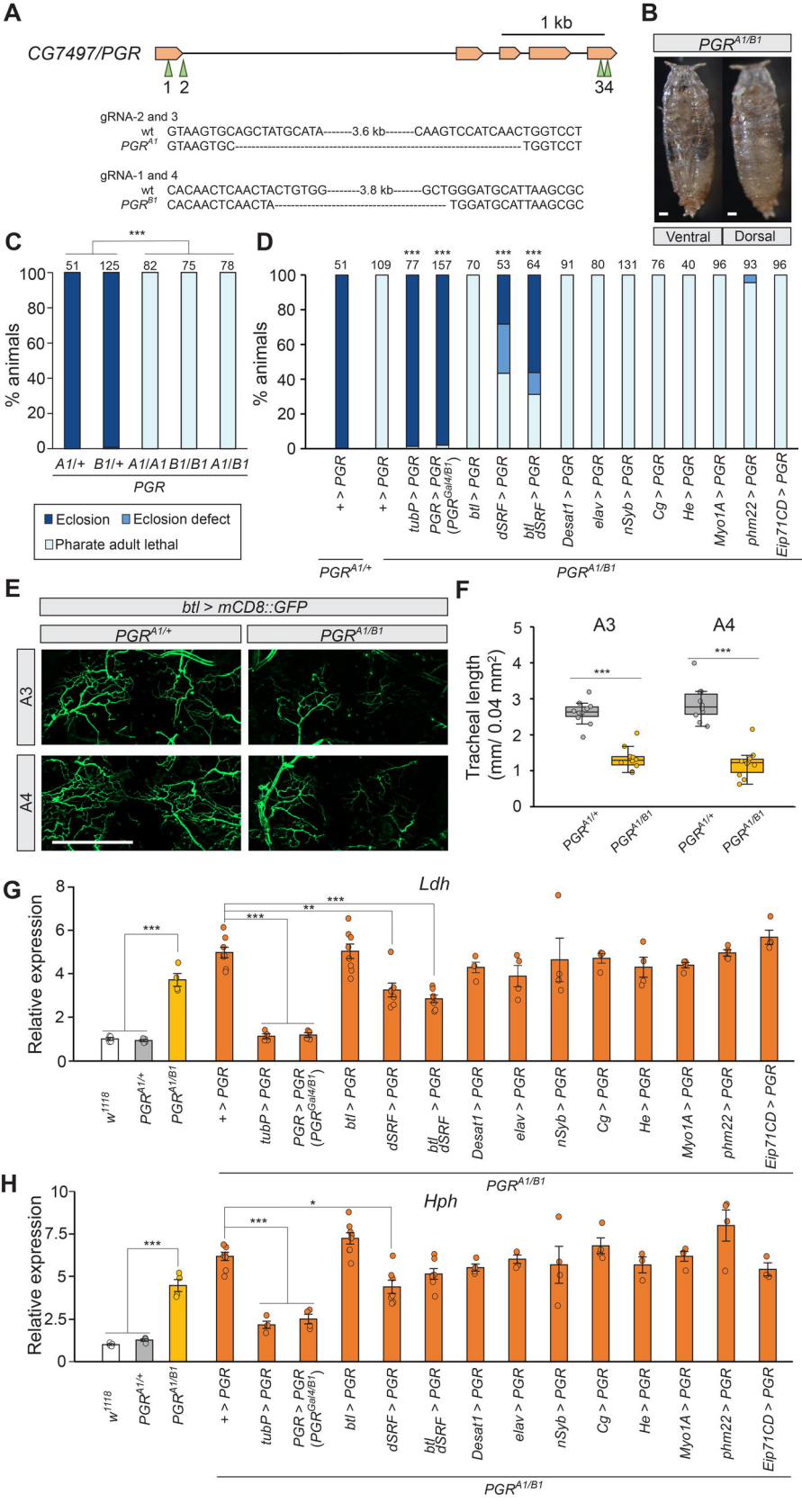
A
CG7497/PGR
1 kb
1 2
34
gRNA-2 and 3
wt GTAAGTGCAGCTATGCATA-------3.6 kb-------CAAGTCCATCAACTGGTCCT
PGRA1 GTAAGTGC----------TGGTCCT
gRNA-1 and 4
wt CACAACTCAACTACTGTGG--------3.8 kb-------GCTGGGATGCATTAAGCGC
PGRB1 CACAACTCAACTA---------- TGGATGCATTAAGCGC
B
PGRA1/B1
Ventral
Dorsal
C
% animals
A1/+
B1/+
A1/A1
B1/B1
A1/B1
PGR
Eclosion
Eclosion defect
Pharate adult lethal
D
% animals
+ > PGR
tubP > PGR
PGR > PGR (PGRGal4/B1)
btl > PGR
dSRF > PGR
btl dSRF > PGR
Desat1 > PGR
elav > PGR
nSyb > PGR
Cg > PGR
He > PGR
Myo1A > PGR
phm22 > PGR
Eip71CD > PGR
PGRA1/+
PGRA1/B1
E
btl > mCD8::GFP
PGRA1/+
PGRA1/B1
A3
A4
F
A3
A4
Tracheal length (mm/ 0.04 mm2)
G
Ldh
Relative expression
w1118
PGRA1/+
PGRA1/B1
H
Hph
Relative expression

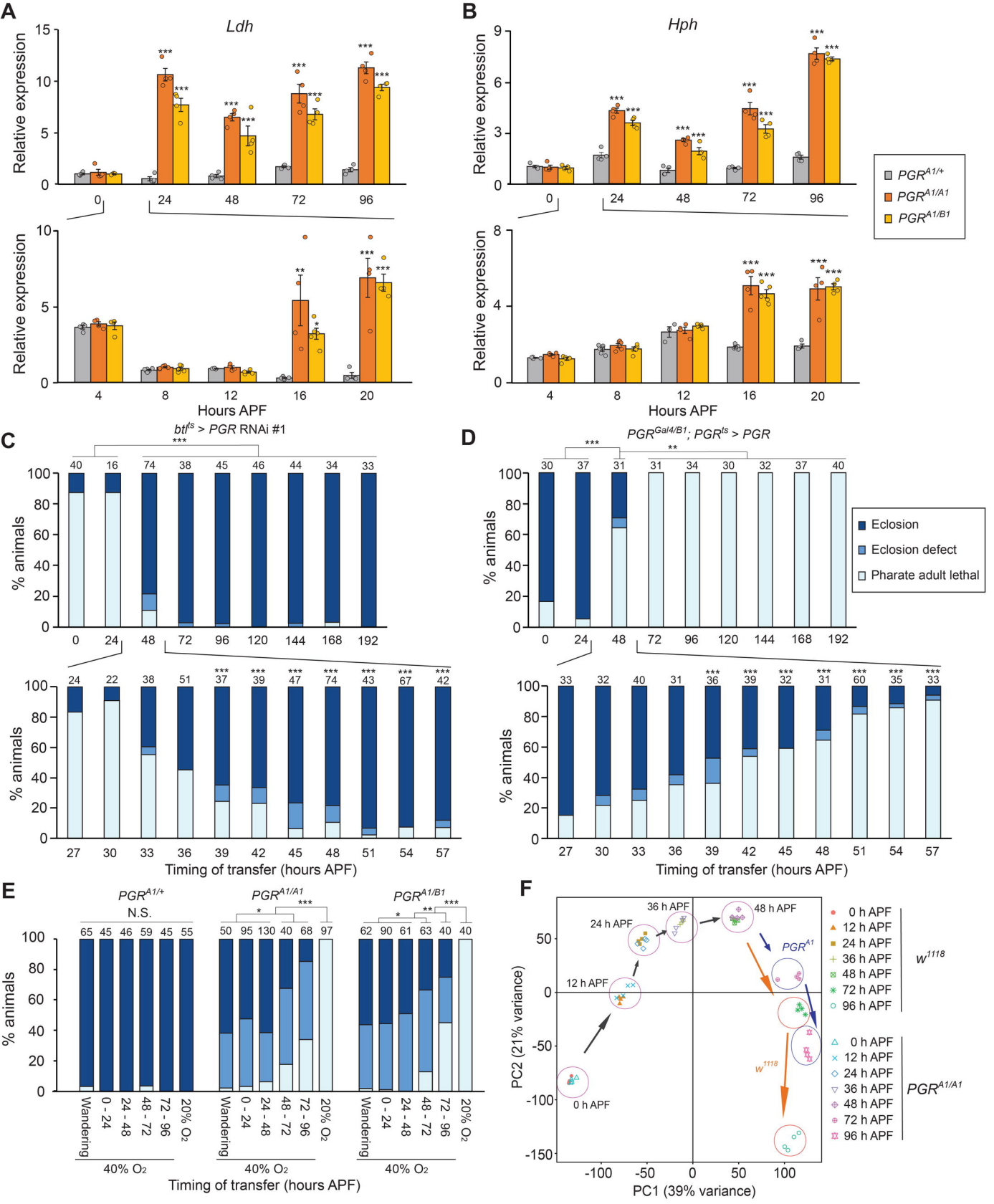
A
Ldh
Relative expression
Hours APF
B
Hph
Relative expression
Hours APF
PGR^A1/+
PGR^A1/A1
PGR^A1/B1
C
btl^ts > PGR RNAi #1
% animals
Timing of transfer (hours APF)
D
PGR^Gal4/B1; PGR^ts > PGR
% animals
Timing of transfer (hours APF)
Eclosion
Eclosion defect
Pharate adult lethal
E
PGR^A1/+
N.S.
PGR^A1/A1
PGR^A1/B1
% animals
Wandering
0 - 24
24 - 48
48 - 72
72 - 96
20% O2
40% O2
Timing of transfer (hours APF)
F
PC1 (39% variance)
PC2 (21% variance)
0 h APF
12 h APF
24 h APF
36 h APF
48 h APF
72 h APF
96 h APF
w^1118
PGR^A1
PGR^A1/A1

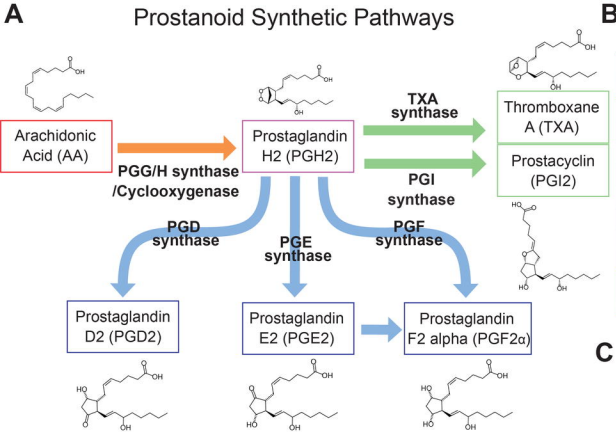

B

Enzyme name in *Homo sapiens*	Function	Group	Orthologs in *Drosophila melanogaster*
Prostaglandin G/H synthase 1/ COX1	AA -> PGH2	Heme Peroxidase	-
Prostaglandin G/H synthase 2/ COX2	AA -> PGH2	Heme Peroxidase	-
Prostaglandin D synthase	PGH2 -> PGD2	Glutathione S-transferase (GST)	GstS1
Prostaglandin-H2 D-isomerase	PGH2 -> PGD2	Lipocalins	-
Prostaglandin E synthase 1	PGH2 -> PGE2	Glutathione S-transferase (GST)	Mgstl, CG33177, CG33178
Prostaglandin E synthase 2	PGH2 -> PGE2	Glutaredoxin domain containing (GLRX)	Su(P)
Prostaglandin E synthase 3	PGH2 -> PGE2	Chaperone	cPges/p23
Prostaglandin F synthase	PGH2 -> PGF2α	Peroxiredoxin	- (*Lepidoptera* has an ortholog)
Prostaglandin F synthase 2	PGH2 -> PGF2α	Aldo-keto reductase	Akr1B?
Carbonyl reductase 1/ PGF synthase	PGE2 -> PGF2α	Carbonyl reductase	- (other insects have orthologs)
Thromboxane A synthase	PGH2 -> TXA	Cytochrome P450 5A1	-
Prostacyclin synthase	PGH2 -> PGI2	Cytochrome P450 8A1	-

C

AA in food (μg/g)	AA (ng/animal)	PGD2 (pg/animal)	PGE2 (pg/animal)	PGF2α (pg/animal)	TXA2 (and metabolites)	PGI2 (and metabolites)
0	0.13 ± 0.063	N.D.	N.D.	N.D.	N.D.	N.D.
500	212.9 ± 24.2	11.3 ± 2.2	8.1 ± 1.1	4.0 ± 0.5	N.D.	N.D.

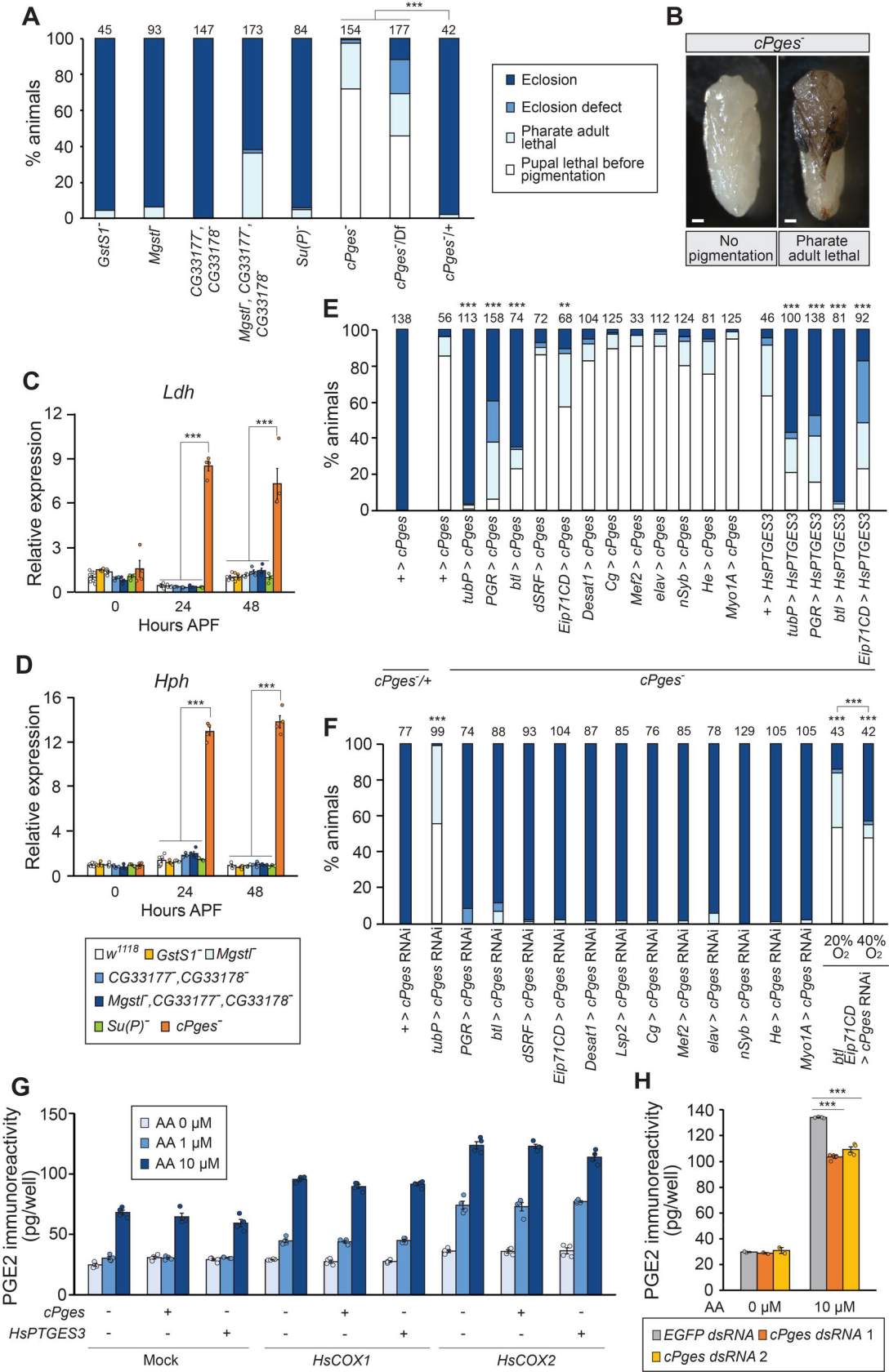
A
% animals
45
93
147
173
84
154
177
42
***
Eclosion
Eclosion defect
Pharate adult lethal
Pupal lethal before pigmentation
GstS1⁻
Mgstl⁻
CG33177⁻, CG33178⁻
Mgstl⁻, CG33177⁻, CG33178⁻
Su(P)⁻
cPges⁻
cPges⁻/Df
cPges⁻/+
B
cPges⁻
No pigmentation
Pharate adult lethal
C
Ldh
Relative expression
Hours APF
D
Hph
w1118
GstS1⁻
Mgstl⁻
CG33177⁻,CG33178⁻
Mgstl⁻,CG33177⁻,CG33178⁻
Su(P)⁻
cPges⁻
E
% animals
+ > cPges
+ > cPges
tubP > cPges
PGR > cPges
btl > cPges
dSRF > cPges
Eip71CD > cPges
Desat1 > cPges
Cg > cPges
Mef2 > cPges
elav > cPges
nSyb > cPges
He > cPges
Myo1A > cPges
+ > HsPTGES3
tubP > HsPTGES3
PGR > HsPTGES3
btl > HsPTGES3
Eip71CD > HsPTGES3
cPges⁻/+
cPges⁻
F
% animals
+ > cPges RNAi
tubP > cPges RNAi
PGR > cPges RNAi
btl > cPges RNAi
dSRF > cPges RNAi
Eip71CD > cPges RNAi
Desat1 > cPges RNAi
Lsp2 > cPges RNAi
Cg > cPges RNAi
Mef2 > cPges RNAi
elav > cPges RNAi
nSyb > cPges RNAi
He > cPges RNAi
Myo1A > cPges RNAi
btl Eip71CD > cPges RNAi
20% O2
40% O2
G
PGE2 immunoreactivity (pg/well)
AA 0 μM
AA 1 μM
AA 10 μM
cPges
HsPTGES3
Mock
HsCOX1
HsCOX2
H
PGE2 immunoreactivity (pg/well)
AA
0 μM
10 μM
EGFP dsRNA
cPges dsRNA 1
cPges dsRNA 2